University of Tartu

Institute of Chemistry

Helen Sepman

Investigation of Fluorescent Reactions in Charged Droplets for Reaction Kinetics Monitoring

Master's Thesis in Materials Science (30 EAP)

Supervisors: Andi Kipper PhD

Anneli Kruve PhD

Tartu 2021

INFORMATION SHEET

Investigation of Fluorescent Reactions in Charged Droplets for Reaction Kinetics Monitoring

Charged droplets is a promising environment to carry out reactions cost-effectively and on accelerated rates. Although, concentration due to evaporation and surface chemistry seem to play an important role in acceleration, the mechanism remains unclarified. One possibility to get insight into reaction kinetics in charged droplets is using laser-induced fluorescence spectroscopy for real-time electrospray investigation, which requires one of the reagents and the product to be fluorescent. Within the scope of this work, four reaction types - imine/hydrazone formation, Katritzky and Zincke reaction were investigated with fluorescent reagents and suitable reactions for reaction kinetics in situ monitoring in electrospray were determined.

Keywords: electrospray ionization, charged droplets

CERS code and names: P300 Analytical Chemistry

Laetud tilkade süntees fluorestseeruvate ühenditega reaktsioonide kineetika uurimiseks

Laetud tilgad on paljulubav keskkond reaktsioonide kiiremaks ning kuluefektiivseks läbiviimiseks. Kuigi aurustumisest tulenev kontsentreerumine ning pinnakeemial on oluline mõju reaktsioonide kiirenemisele, pole kiirenemise mehhanism täpselt teada. Üheks võimaluseks tilkade uurimiseks on kasutada laser-indutseeritud fluorestsentsspektroskoopiat, mis võimaldab reaalajas reaktsioonikineetika uurimist, kui vähemalt üks lähteaine ning produkt on fluorestseeruvad. Käesoleva töö raames uuriti nelja reaktsioonitüüpi – imiini/hüdrasooni teket, Katritzky ja Zincke reaktsiooni kasutades fluorestseeruvaid lähteaineid ning leiti sobivad reaktsioonid laetud tilkade kineetika edasiseks uurimiseks.

Märksõnad: elektrosprei ionisatsioon, laetud tilgad

CERS kood ja nimetus: P300 Analüütiline Keemia

Table of Contents

Abbreviations

µL	microliter
EASI	easy ambient sonic-spray ionization
ES	electrospray
ESI	electrospray ionization
ESSI	electrosonic spray ionization
EtOH	ethanol
kV	kilovolt
LC	liquid chromatography
LIF	laser-induced fluorescence
MeCN	acetonitrile
MS	mass-spectrometry
ND	not determined
nESI	nano electrospray ionization
NMR	nuclear magnetic resonance
NR	no reaction
UV	ultraviolet
UV-Vis	ultraviolet-visible light

1. Introduction

Chemical synthesis plays a crucial role in production for variety of industries. In order to optimize production, reactions are often carried out with the help of a catalyst or using elevated temperatures, yet can still be time- and resource-consuming. Hence, constant development of new catalysts and techniques is required.

Recently, charged droplets have attracted attention as an alternative environment to carry out reactions. Compared to bulk reactions, acceleration rates up to six orders of magnitudes have been observed which makes it promising method to increase efficiency of production while reducing the consumption of solvents, reagents and reaction time.

Although, contributing effect of solvent evaporation, increased concentrations of reagents and ions as well as high surface-volume ratio have been considered to play a key role in many cases, the exact acceleration mechanisms remain unknown. Understanding occurring processes in charged droplets would be beneficial to predict suitability for various applications and optimize their use as a reaction environment. Due to dynamic heterogeneous environment, short lifetime of the droplets and limited techniques for investigation, reaction monitoring directly in spray has received little attention and information of reaction kinetics is often obtained by using analytical techniques such as mass spectrometry.

The aim of this work is to determine reactions with suitable fluorescence properties and reaction speed to provide insight into reaction kinetics and mechanisms in charged droplets with further aim to performing in situ laser induced fluorescence spectroscopy experiments. For that, fluorescence of one reagent and the product with different emission spectra maxima is needed to observe the evolution of the reaction along the spray. Imine/hydrazone formation, Zincke and Katritzky reactions with fluorescent reagents and potentially fluorescent products are studied in charged droplets, corresponding bulk reactions are conducted and conversion rates are assessed.

The gathered information helps us further understand the processes occurring in droplets and allows us to optimize reaction parameters for widescale use of charged droplets as environment to carry out syntheses on accelerated rates.

2. Literature Overview

Continuous research in the field of organic synthesis is carried out in order to discover alternative reaction routes improving the consumption of time and resources. Over the past decade, microdroplets have shown promise as reaction environments providing accelerated reaction rates and improved yields. Simplicity of the method and increase in reaction rates compared to bulk reactions makes it a promising subject for further investigation.

2.1. Reactions in Confined Spaces

Interest in microscale compartmentalization has grown over past few decades with the motivation to minimize solvent and reagent consumption, have better control over reaction and carry out high throughput research. Wide range of confined environments, such as aerosols[1], emulsions[2], acoustically[3] and Leidenfrost[4,5] levitated droplets, surface drop-casting[6], thin films[7], on-water/two phase interfaces[8] and micelles[9], have found use as catalytic systems. Recently, number of reactions have been reported to occur up to six orders of magnitudes faster compared to bulk reactions which has shifted the focus towards acceleration of reactions.[9–11]

The thermodynamic and kinetic properties in neutral confined spaces differ from bulk and enhancements in reaction rates have been demonstrated. Acceleration rate of 45 times has been reported in aldehyde and amine reaction producing imine on the interface of immiscible organic and water phase in microfluids.[12] In Leidenfrost droplets, where the droplet is levitated on its solvents vapour cushion, the reaction rates have been accelerated up to 200 times.[4,5] It was noticed that the bromo-substituted pyridines gave higher yields than iodo-substituted reagents which is also the trend in bulk reactions and indicates that reactions in droplets may proceed through the same reaction pathways as in bulk.[5] Similarly, acoustically levitated droplets as reaction medium have shown slight enhancement in reaction rates. Acid-catalysed degradation of antibiotic erythromycin A with 5% of formic acid occurred at least an order of magnitude faster.[3]

Even higher acceleration rates have been observed using electrospray ionization based methods that produce charged droplets by electrohydrodynamic tip streaming.[10] Furthermore, conducting reactions in charged confined environments can have number of advantages over neutral micellar systems, such as simpler product extraction and scale-up of production.[9,10] This work focuses on charged droplets as an environment to carry out reactions and their properties are discussed in further chapters.

2.2. Reactions in Charged Droplets

Electrospray ionization is an ionization source mainly used in mass-spectrometry (MS) where analyte is pumped through a capillary needle at low flow rate (0,1-10 µL/min) and a high positive or negative voltage (2-5 kV) is applied to produce charged droplets from which gas-phase ions are emitted for MS analysis.[13] Several models have been proposed to describe the location of ions in ESI droplets. The charge residue model proposes that as the solvent evaporates the charge density increases which causes the fission of droplets and smaller droplets are produced. This process can occur a number of times until dry single ions are left. By ion evaporation model, low molecular weight ions exist on the surface of droplets being partially solvated at the air-droplet interface and dry ions are ejected by Coulombic forces.[13,14] However, occurring processes likely depend on used solvent, chemicals and ambient conditions. Several methods containing electrospray as an ionization source (Table 1) have shown acceleration of reactions for formation of heterocyclic compounds[11,15], aldol reaction[16], cycloaddition[17], transamination[18], elimination[19], phosphorylation[20,21] and multicomponent reactions[22,23].

Pomeranz-Fritsch synthesis of isoquinoline, a widely used precursor in pharmacy, can take up to days and needs high temperature and acid catalyst in bulk. On the contrary, reaction conducted in charged droplets produced by electrospray ionization (ESI) yielded product in millisecond timescale proposing possible applications on the field of pharmacy for the charged droplets.[11] Similarly, tert-butyloxycarbonyl group that is broadly used to protect amino functional groups in multistep synthesis and needs relatively strong acids and/or heat to be removed, resulted acceleration of two orders of magnitude in previously acidified charged droplets using easy ambient sonic-spray ionization (EASI).[19] Furthermore, thermodynamically unfavoured reaction in bulk - phosphorylation of saccharides has been reported to occur in charged microdroplets, suggesting prebiotic reactions in aqueous microdroplets produced by breaking waves, waterfalls and clouds as a feasible theory for origin of life.[20,21]

Although (physical) mechanisms of reaction acceleration are not fully understood it has been proposed based on experimental data that the main factors contributing to the latter are solvent evaporation causing the increased concentration of reagents and charges in the droplets as well as confinement in spaces with high surface-to-volume ratio.

As the droplets shrink and reagents become more concentrated, more intermolecular collisions occur resulting reaction rate acceleration. It has been demonstrated that the reaction rates correlate to the evaporation rates of the respective solvents.[6] During evaporation, ions carrying

a charge also become more concentrated. In an aqueous solution, the main contributors to droplet net charge are protons produced by electrolytic water oxidation ($2\ H_2O \rightarrow 4\ H^+ + 4e^- + O_2$) on metal-solution interface of the capillary.[14,24] Decrease in pH up to four units has been observed in charged droplets and implemented in studies of pH-responsive protein folding.[10,25] Additionally, acid and base catalysed reactions in positive and negative modes respectively have been accelerated.[26]

Depending on electrospray conditions, concentration by evaporation may require increased distance between the electrospray source and counter electrode as longer distance results more time for the solvent to evaporate and increases the reaction time. Altering the distance between capillary tip and counter electrode for multi-step Hantzsch reaction resulted in significant changes in product distribution analysed with MS.[22] However, discontinuities in solvent evaporation, such as complete solvent evaporation or ejection of ion from the droplet by Coulombic forces, terminate the reaction as the reaction is considered to occur until gas-phase ions are emitted.[13,14] Although, gas-phase reactions are also possible, they usually do not produce enough product for practical applications.[15] Fischer Indole synthesis, where different products are produced depending on whether the reaction is carried out in gas- or liquid-phase, has been investigated for droplet reactions. Results suggested solution phase reactions as liquid-phase product was formed in charged droplets.[15][15] For continuous evaporation distance, temperature and droplet-formation conditions, such as size of the initial droplet, can be controlled and altered by capillary tip diameter, applied voltage, sheath gas pressure and flow rate.[10,27].

Main differences in physical properties between the accelerated reactions in droplets from corresponding bulk reactions are the reduced volumes and increased surface areas. Polar surface environment is likely to play a dominant role in contribution to acceleration. As ions at the air-droplet interface are not completely solvated and have incomplete solvent shell, reduced desolvation energy is required for the collision of reagents to occur. In comparison, in bulk solutions large solvation-energy barriers must be overcome for the reaction to occur which lowers the reaction rate. Meanwhile, partly solvated ions can overcome activation barriers more easily. It was demonstrated that when reaction was electrostatically forced to occur inside the thin film instead of air-droplet interface the reaction rate decreased.[7] Aqueous solutions of cytochrome c and maltose acid-catalysed reaction yielded higher rates in droplets than in bulk although evaporation was very little suggesting that concentration is not the only source of reaction acceleration and the droplet-air interface plays an important role.[28] The use of

surfactant that blocks the air-droplet interface in the Leidenfrost droplets in Claisen-Schmidt reactions also resulted suppression of acceleration by a few factors which supports the theory of importance of surface interactions.[4]

Table 1. Selected examples of reactions that have been accelerated with different methods of electrospray ionization to produce charged droplets.

Reaction	Scheme	Method
Pomeranz-Fritsch synthesis of isoquinoline[11]	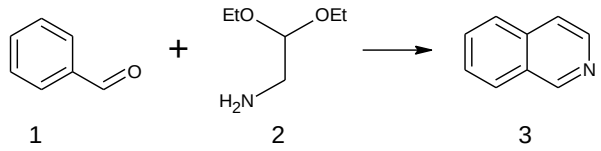 1 2 3	ESI
Claisen-Schmidt condensation[16]	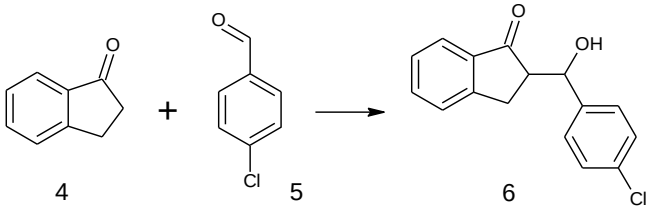 4 5 6	ESSI
Fischer Indole synthesis[15]	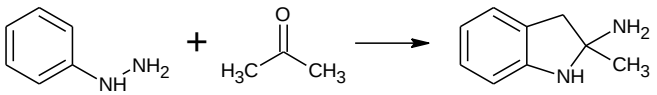 7 8 9	nESI
Katritzky reaction[18]	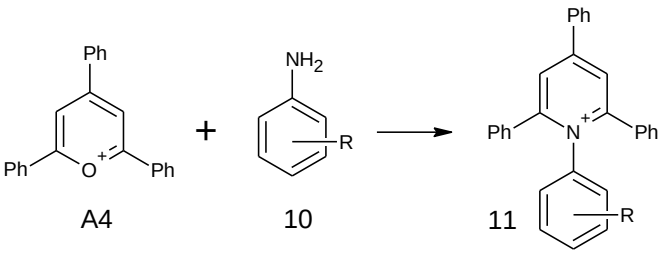 A4 10 11	Reactive paperspray

2.2.1. Importance of Investigating Microdroplets

Charged microdroplets are prospective environment to carry out organic synthesis. They can be used to speed up bulk-phase reactions and produce high yields of product, possibly with simplified work-up (if solvent and reagents are volatile) and more economically feasible production process. Speeding up the reactions allows rapid analysis as well as high-throughput research and the process is easy to scale up by simply using more capillaries to carry out reactions.

Charged droplets follow the trend of environmentally friendlier solutions and guidelines of green chemistry by reducing energy, solvent and chemicals consumption.[9] For many reactions that need acid/base to carry out the reaction with reasonable reaction rate in bulk have yielded product in absence of catalyst in charged droplets.

The simplicity and generality of the microdroplets makes it applicable in wide range of reactions. They can be used to produce nanoparticles[29,30] and polymers[31] as well as they have been successfully implemented in drug discovery to study the stability of pharmaceuticals[3,32] and synthesise drug precursors[11,15]. Confined environments have been proposed as possible origin of life[20,21] and could give insight to biochemical processes, be used to mimic cells and carry out environmental studies.

2.3. Profiling Reactions with Laser-Induced Fluorescence Spectroscopy

Information about reaction kinetics is often obtained from mass spectrometry (MS) analysis by measuring the signal intensity of the products. Reaction time can be calculated by knowing the distance between capillary and counter electrode.[27,33] However, this method does not provide real-time information of processes occurring in charged droplets and might require corrections based on ionization efficiencies of the substances. In order to get better insight into droplet evolution and reaction progress, in situ measurements with laser can be performed.

Laser-induced fluorescence (LIF) spectroscopy is an analytical technique used for exciting a small volume of molecules with the help of a laser and measuring emission spectrum at 90° to the laser beam (Fig. 1).[34] Due to high sensitivity and precision of LIF, it has provided valuable information about processes in electrospray. Using fluorescent pH indicator carboxyseminaphthorhodafluor-1 axial profiling of the spray has been performed in both positive and negative mode to investigate acidic/basic properties.[35] Similarly, solvent polarity has been investigated with fluorescent solvatochromic dyes, where red shift (8-12 nm) indicated increase in polarity moving further from the needle.[36] Additionally, as temperature can affect solute chemistry (conformation, solvent evaporation, fractionation process, kinetics, equilibria), evolution of droplet temperatures in electrospray plume have been investigated using rhodamine dyes that have temperature-induced shift in emission spectrum.[37,38]

In order to get quantitative data from LIF experiments of dispersed spray, internal standards are often used. However, if one of the reagents and the product are fluorescent and have significantly different emission spectra maxima, product formation can be assessed in respect

to the reagent based on their fluorescence signals intensities. Developing a method based on ratio of fluorescence signals is crucial to compensate for signal loss in dispersed spray. Exploring this type of reactions would give valuable insight into reaction evolution in charged droplets and occurring processes as well as possibility to monitor the reaction kinetics in situ along the spray.

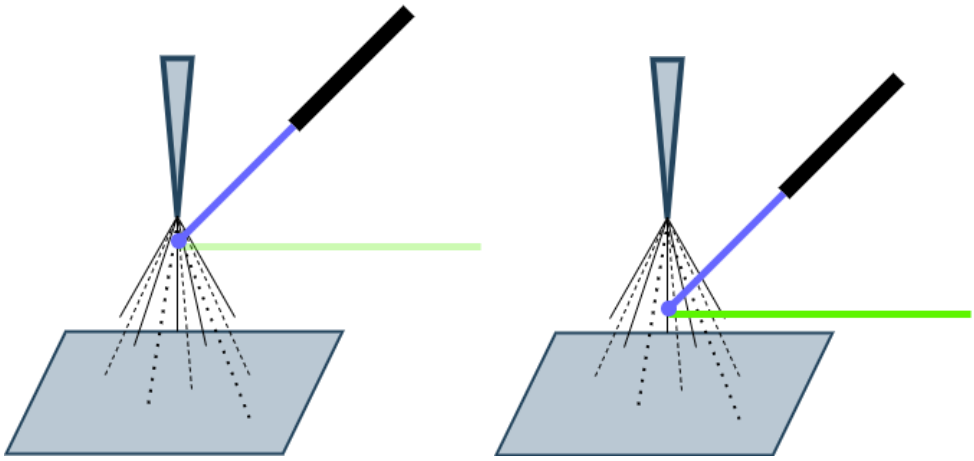

Figure 1. LIF experiment setup. Small area of spray is excited with laser and emission spectrum is acquired. By measuring points at different distances from the needle along the spray it is possible to obtain information of the evolution of spray reaction.

2.4. Investigated Reaction Types

Reactions investigated in this work can be divided to four groups based on the reaction types (Table 2). The following reactions were chosen as they are relatively slow reactions under ambient conditions and require a catalyst for reasonable reaction times. Imine/hydrazone formation is acid-catalysed reaction, which have demonstrated high acceleration rates in positive electrospray (ES) mode. Zincke and Katritzky reactions that have high potential to extend the conjugated system and result a fluorescent product if suitable reagents are chosen. Reaction types were investigated using different reagents to determine reactions with suitable conversions and fluorescence properties of the reagent and the product.

Table 2. Reactions types investigated in this work.

Imine formation[39]	Acid-catalysed reaction between amine and aldehyde produces imine.	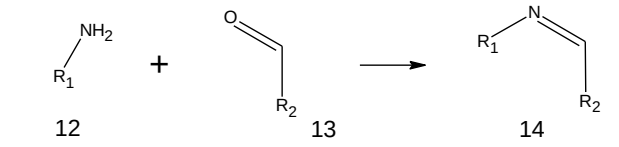 12 13 14
Hydrazone formation[40]	Acid-catalysed reaction between hydrazine and aldehyde produces hydrazone.	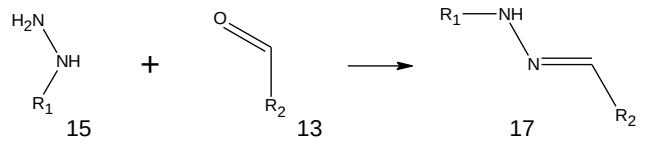 15 13 17
Zincke reaction[41]	Pyridine is transformed to a pyridinium salt with 2,4-dinitrochlorobenzene and primary amine.	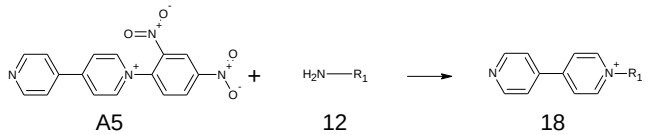 A5 12 18
Katritzky reaction[4,18]	Reaction between pyrylium salt and functionalized primary amine.	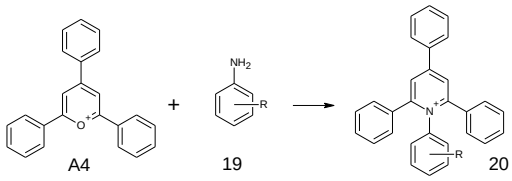 A4 19 20

3. Materials and Methods

3.1. Reagents and Solvents

Reagents used to carry out reactions in charged droplets: 1-pyrenecarboxaldehyde (Alfa Aesar, 99%), 9-anthracenecarboxaldehyde (Sigma-Aldrich, 97%), cinnamaldehyde (Sigma-Aldrich, 99%), 2,4,6-triphenylpyrylium tetrafluoroborate (Sigma-Aldrich, 98%), 4-aminobiphenyl (Sigma-Aldrich, ≥98%), 2-aminofluorene (Sigma-Aldrich, 99%), phenylhydrazine (Sigma-Aldrich, 97%). Structural information, average molar mass and fluorescence emission information can be found in a table in SI 1.

Reagents 4,4'-bipyridine (Sigma-Alrich, 99%) and 1-chloro-2,4-dinitrobenzene (Alfa Aesar, 98%) were used to synthesize Zincke reaction reagent 1-(2,4-dinitrophenyl)-4-(pyridine-4-yl)pyridinium chloride (SI 2).

Solvents used to prepare reagent solutions: Acetonitrile (Sigma-Aldrich, LC-MS grade), ethanol (Honeywell Riedel-de Haën, 99.8%).

Solvents and reagents used for LC-MS analysis: acetonitrile (Sigma-Aldrich, LC-MS grade), Formic acid (Honeywell, ≥98%) and MilliQ water (purified with in-house system).

Deuterated dimethyl sulfoxide-d6 (Deutero, 99.8% D) and deuterated chloroform-d (Deutero, 99.8% D) were used as solvents for NMR analysis. Additionally, deuterated methanol-d4 (Deutero, 99.8% D) was used to monitor the kinetics with NMR.

3.2. Electrospray System

In-house built electrospray system was used to carry out reactions. The system was placed into ventilated transparent box made out of poly(methyl methacrylate) for safety. Additionally, infusion pump and metal parts of the system were grounded.

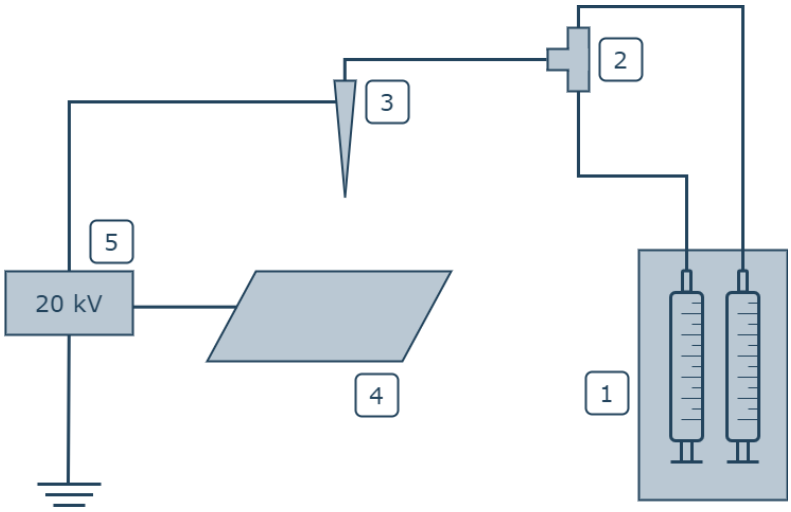

Figure 2. The scheme of electrospray system used to carry out reactions.

1. Infusion pump with two syringes containing solutions of reagents

2. PEEK tubing and T-junction

3. Electrospray needle/capillary

4. Counter electrode (stainless steel plate)

5. High voltage power supply (up to 20 kV)

Two reagent solutions were infused from separate syringes with flow rates of 8-16 µL/min to the PEEK tubing. After T-junction, reagents were mixed (dead volume of mixing PEEK tubing approx. 10 µL) and sprayed from electrospray needle under high voltage (7.7 - 15.7 kV) that was tuned until fine spray was achieved (confirmed visually by illuminating the spray from back with light). The distance between capillary and plate were pre-optimized and kept approximately constant (distances from 103 to 135 mm were used).

3.3. Instrumentation for Analysis

Agilent Series 1100 liquid chromatograph coupled to LC/MSD Trap XCT ion trap mass spectrometer (Santa-Clara, USA) with ESI source and Agilent 1290 Infinity series liquid chromatograph coupled to Agilent 6495 Triple Quad LC/MS (Santa-Clara, USA) with ESI source were used to analyse reaction mixtures and assess the conversions of reactions. Both LC instruments were equipped with binary pump, autosampler, thermostated column compartment and diode array detector. Agilent ChemStation for LC Rev. A. 10.02 and MSD Trap Control

version 5.2 were used for Agilent XCT and MassHunter Workstation LC/MS Data Acquisition for 6400 Series Triple Quadrupole Version B.07.00 for Agilent QQQ instrument were used to control the instrument. The column used was Kinetex (100 x 3.00 mm, particle size 2.6 µm). Eluent system 0.1% formic acid in MQ water/MeCN with flow rate 0.8 mL/min was used for gradient elution as follows: 5% of MeCN was held for 5 minutes, increased up to 100% by 10th minute and held until 15th min, then decreased to 5% by 20th minute.

DataAnalysis for LC/MSD Trap version 3.2 and Qualitative Analysis version B.07.00 programs were used for post-analysis of LC-MS experiments results. Conversion was assessed from LC-MS UV-chromatograms at absorption wavelength of 254 nm and calculated as percentage of product's peak area of the sum of one reagent and product peaks' areas. The reagent peak was chosen based on peak shape, stability and similarity of the chromophoric groups.

Fluoromax-4 (HORIBA Jobin Yvon) fluorescence spectrometer was used to measure emission spectra of reagents and reaction mixtures to confirm new emission peaks. Measurement parameters used to acquire emission spectra: excitation wavelength used for different measurements was in range of 280-360 nm, emission spectra acquisition started at 20 nm longer wavelength of the respective excitation wavelength and was measured up to 700 nm with increment of 1 nm, slit size of 2 nm was used both entrance and exit slits.

Bruker Ascend nuclear magnetic resonance (NMR) spectrometer was used operating at 700 MHz to acquire ^{1}H spectra to confirm synthesis products and for real-time kinetics monitoring. Chemical shifts are reported in parts per million (ppm). Bruker TopSpin 3.2 program was used to process measured spectra.

3.4. General Procedure to Carry Out Reactions

To carry out electrospray (ES) reaction, reagent solutions with concentrations of approx. 0.03 M were prepared (slight variance depending on solubility) by weighing reagents into two separate 4 mL vials and adding 2 mL of solvent (MeCN or EtOH). The complete dissolution took place. Two syringes were filled with each reagent solution, connected to PEEK tubing and placed on the infusion pump. The system was purged with 2x100 µL of solutions. A grounded plate was added to the system and distance from the needle to the plate was marked down (in the range of 103 to 135 mm). Infusion pump and the voltage were turned on, the spray was illuminated from back with a lamp and the flow rate and voltage were tuned until the spray was visually well dispersed (flow rate used was in the range of 8 to 16 µl/min and voltage 7.7 to

15.7 kV). After infusing 2x200 µL of solutions, voltage and flow were turned off and the substances on the plate were washed into a 4 mL vial with approx. 1 mL of previously used solvent. Samples for LC-MS were prepared immediately by diluting the solution approximately 100 times. The syringes were washed three times with ethanol and the system was purged with 2x700 µL of ethanol.

To carry out reference bulk reaction, 200 uL of both reagent solutions (prepared in the previous step) were pipetted to a 4 mL vial. The reaction was let to occur for 60 seconds and LC-MS samples were prepared immediately by diluting the solution approximately 100 times.

3.5. Rate law and method of initial rates

The rate law is expressed as:

$$v = k \times [A]^x \times [B]^y \tag{1}$$

Where *v* corresponds to average rate of the reaction, *k* to kinetic constant, [A] and [B] are concentrations of reagents and x and y are orders of reaction in respect to reactants.

To determine the reaction rate and kinetic constant, method of initial rates was followed. Initial rate of reaction is obtained from the beginning of the reaction where the product formation can be described with a linear regression model. The rate is measured for several initial concentrations and altering one concentration at the time, parameters for kinetics can be calculated. When two measurements are done keeping concentration of reagent A constant, the quotient of the rate laws can be expressed as:

$$\frac{v_2}{v_1} = \frac{\cancel{k \times [A]_1^x} \times [B]_2^y}{\cancel{k \times [A]_1^x} \times [B]_1^y} \tag{2}$$

By taking logarithm from both sides we can find the reaction order y in respect of reactant B:

$$y = \frac{\log\left(\frac{v_2}{v_1}\right)}{\log\left(\frac{[B]_2}{[B]_1}\right)} \tag{3}$$

Similarly, reaction order in respect of reactant A can be obtained. The overall reaction order can be calculated as the sum reactions orders in respect of the reactants (overall reaction order

= x + y). When reaction orders are determined, kinetic constant can be calculated from the rate law.

4. Results and Discussion

4.1. LC-MS Analysis of Droplet and Bulk Reactions

Eleven reactions in charged droplets produced by ES and corresponding bulk reactions were carried out. To assess conversions of both reactions, LC-MS measurements were performed for approx. 100x diluted reaction mixtures. One measurement was performed to most of the reactions with a few exceptions of two measurements.

Results presented below are divided into paragraphs by reaction types: imine/hydrazone formation, Katritzky and Zincke reactions, in respective order. Reaction scheme is presented for each reaction with expected product followed by summary table consisting of calculated monoisotopic mass of molecular ion [M+H] (cation mass for salts), detected *m/z* value and retention time for reagents and product (if detected). Additionally, reaction conversions in ES and bulk reactions are assessed based on UV-chromatograms which can be found in SI 4. It is assumed that molar extinction coefficients of reagents and product are similar, and the difference in absorptions is not relevant in the context of this work. For reactions that did not occur, no reaction (NR) is marked. Reactions that occurred based on MS yet the conversion could not be assessed are marked as not determined (ND). All obtained results are summarised in Table 14.

4.1.1. Imine/Hydrazone Formation Reactions

4.1.1.1. Reaction Between 1-Pyrenecarboxaldehyde (A1) and 2-Aminofluorene (B2)

Figure 3. Reaction scheme of A1 and B2 with expected product C2.

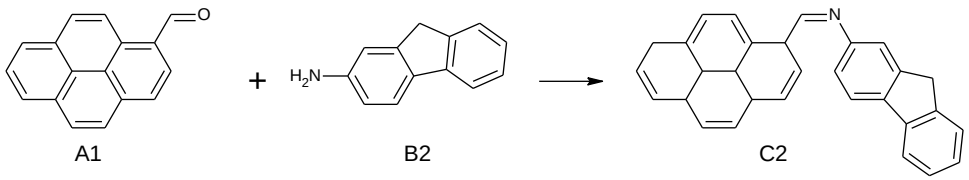

Table 3. Summary table of reaction between A1 and B2.

	A1	**B2**	**C2**
Monoisotopic mass [Da]	231.08	182.10	394.16
Detected [*m/z*]	230	182	-
Retention time R_t [min]	6.5	4.1	-
Conversion in ES (%)	-	-	NR
Conversion in bulk (%)	-	-	NR

Pyrenealdehyde did not yield a peak in UV chromatogram. However, signal of the reagent with low intensity could be observed in MS spectrum. New peaks in UV-chromatogram for the expected *m/z* of the product were not observed.

4.1.1.2. Reaction between 1-Pyrenecarboxaldehyde (A1) and Phenylhydrazine (B3)

Figure 4. Reaction scheme of A1 and B3 with expected product C3.

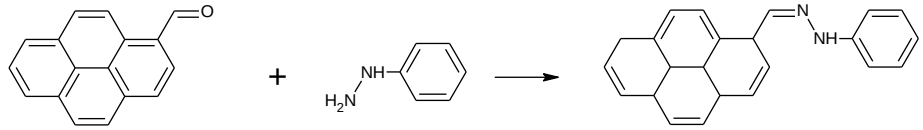

A1 B3 C3

Table 4. Summary table of reaction between A1 and B3.

	A1	**B3**	**C3**
Monoisotopic mass [Da]	231.08	109.08	321.14
Detected [*m/z*]	231	109	321
Retention time R_t [min]	12.6	Dead time	13.9
Conversion in ES (%)	-	-	3-10
Conversion in bulk (%)	-	-	NR

4.1.1.3. Reaction between 9-Anthracenecarboxaldehyde (A2) and 4-Aminobiphenyl (B1)

Figure 5. Reaction scheme of A2 and B1 with expected product C4.

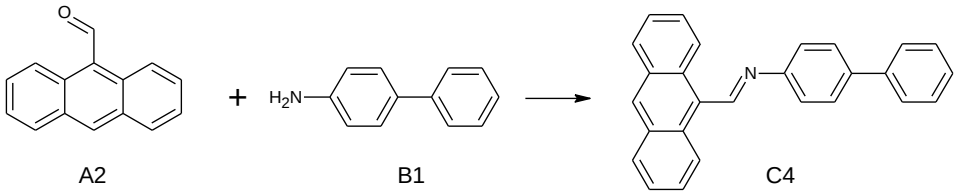

A2 B1 C4

Table 5. Summary table of reaction between A2 and B1.

	A2	**B1**	**C4**
Monoisotopic mass [Da]	207.08	170.10	358.16
Detected [*m/z*]	209	170	-
Retention time R_t [min]	6.4	3.6	-
Conversion in ES (%)	-	-	NR
Conversion in bulk (%)	-	-	NR

4.1.1.4. Reaction between 9-Anthracenecarboxaldehyde (A2) and Phenylhydrazine (B3)

Figure 6. Reaction scheme of A2 and B3 with expected product C6.

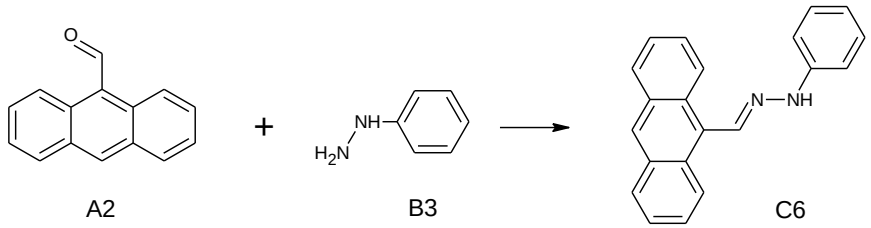

Table 6. Summary table of reaction between A2 and B3.

	A2	**B3**	**C6**
Monoisotopic mass [Da]	207.08	109.08	297.14
Detected [*m/z*]	207	109	297
Retention time R_t [min]	6.3	Dead time	7.7
Conversion in ES (%)	-	-	13 - 63
Conversion in bulk (%)	-	-	NR

4.1.1.5. Reaction between Cinnamaldehyde (A3) and 4-Aminobiphenyl (B1)

Figure 7. Reaction scheme of A3 and B1 with expected product C7.

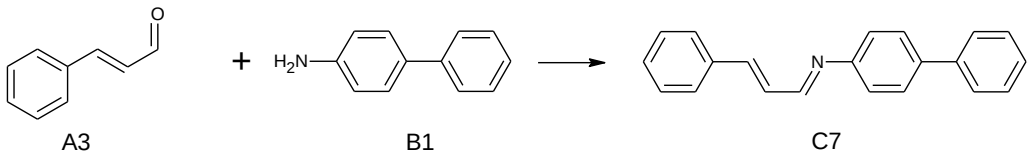

Table 7. Summary table of reaction between A3 and B1.

	A3	**B1**	**C7**
Monoisotopic mass [Da]	133.06	170.10	284.14
Detected [*m/z*]	133	170	-
Retention time R_t [min]	4.2	3.5	-
Conversion in ES (%)	-	-	NR
Conversion in bulk (%)	-	-	NR

4.1.1.6. Reaction between Cinnamaldehyde (A3) and Phenylhydrazine (B3)

Figure 8. Reaction scheme of A3 and B3 with expected product C9.

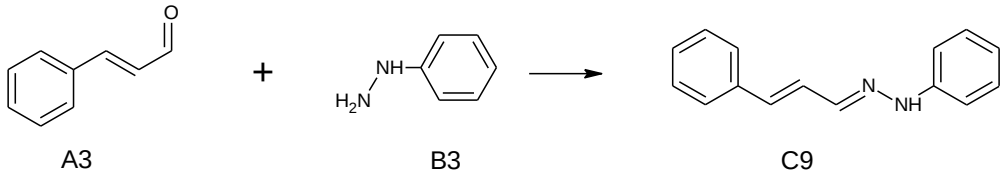

Table 8. Summary table of reaction between A3 and B3.

	A3	**B3**	**C9**
Monoisotopic mass [Da]	133.06	109.08	223.12
Detected [*m/z*]	133	109	223
Retention time R_t [min]	3.9	Dead time	6.6
Conversion in ES (%)	-	-	ND*
Conversion in bulk (%)	-	-	7

* Conversion could not be determined for ES reaction as both reagents are volatile and evaporate in the spray. Reaction has occurred in both ES and bulk reactions.

4.1.2. Katrizky Reactions

4.1.2.1. Reaction between 2,4,6-Triphenylpyrylium Tetrafluoroborate (A4) and 4-Aminobiphenyl (B1)

Figure 9. Reaction scheme of A4 and B1 with expected product C10.

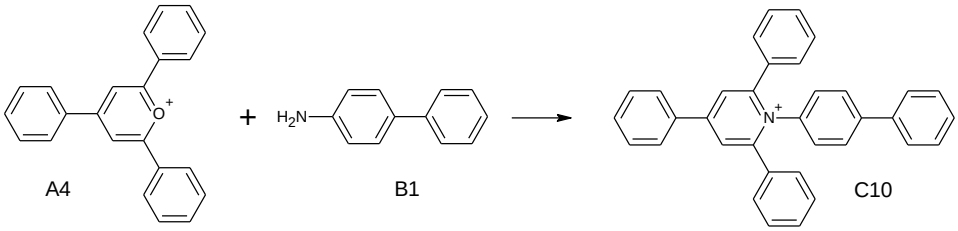

Table 9. Summary table of reaction between A4 and B1.

	A4	**B1**	**C10**
Monoisotopic mass [Da]	309.13	170.10	460.21
Detected [*m/z*]	309	170	460
Retention time R_t [min]	5.7	4.1	7.1
Conversion in ES (%)	-	-	ND*
Conversion in bulk (%)	-	-	NR

* Due to low concentrations of the samples and overlapping peaks in UV-chromatogram, conversion could not be assessed. Based on MS spectra, reaction had occurred in ES but not in bulk reaction.

4.1.2.2. Reaction between 2,4,6-Triphenylpyrylium Tetrafluoroborate (A4) and 2-Aminofluorene (B2)

Figure 10. Reaction scheme of A4 and B2 with expected product C11.

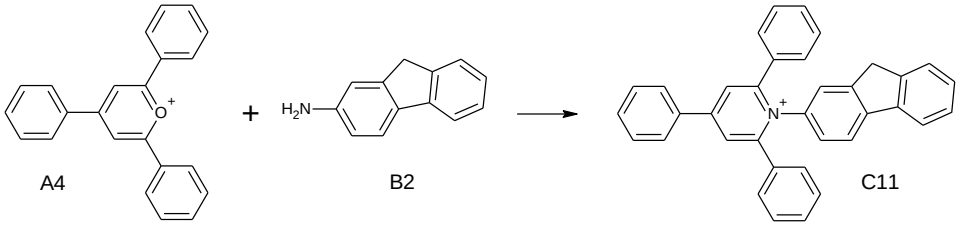

Table 10. Summary table of reaction between A4 and B1.

	A4	**B2**	**C11**
Monoisotopic mass [Da]	309.13	182.10	472.21
Detected [*m/z*]	309	181	472
Retention time R_t [min]	8.1, 11.7*	7.7	9.5
Conversion in ES (%)	-	-	24
Conversion in bulk (%)	-	-	NR

* Reagent A4 decomposed in LC system and yielded multiple peaks in UV-chromatogram.

4.1.3. Zincke Reactions

4.1.3.1. Reaction between 1-(2,4-dinitrophenyl)-4-(pyridine-4-yl)pyridinium chloride (A5) and 4-Aminobiphenyl (B1)

Figure 11. Reaction scheme of A5 and B1 with expected product C13.

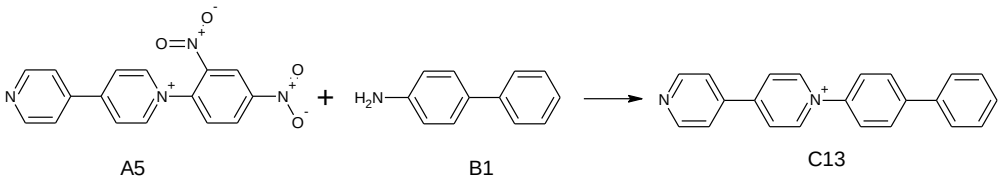

Table 11. Summary table of reaction between A5 and B1.

	A5	**B1**	**C13**
Monoisotopic mass [Da]	323.08	170.10	309.14
Detected [*m/z*]	323	170	309
Retention time R_t [min]	3.2	5.2	5.7
Conversion in ES (%)	-	-	9-22
Conversion in bulk (%)	-	-	1-5

4.1.3.2. Reaction between 1-(2,4-dinitrophenyl)-4-(pyridine-4-yl)pyridinium chloride (A5) and 2-Aminofluorene (B2)

Figure 12. Reaction scheme of A5 and B2 with expected product C14.

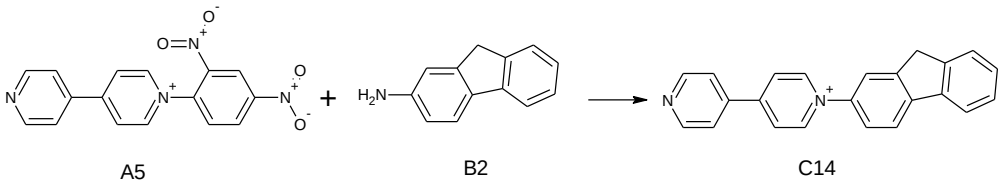

Table 12. Summary table of reaction between A5 and B2.

	A5	**B2**	**C14**
Monoisotopic mass [Da]	323.08	182.10	321.14
Detected [*m/z*]	323	182	321
Retention time R_t [min]	3.5	5.3	5.8
Conversion in ES (%)	-	-	14-58
Conversion in bulk (%)	-	-	2-24

4.1.3.3. Reaction between 1-(2,4-dinitrophenyl)-4-(pyridine-4-yl)pyridinium chloride (A5) and Phenylhydrazine (B3)

Figure 13. Reaction scheme of A5 and B3 with expected product C15.

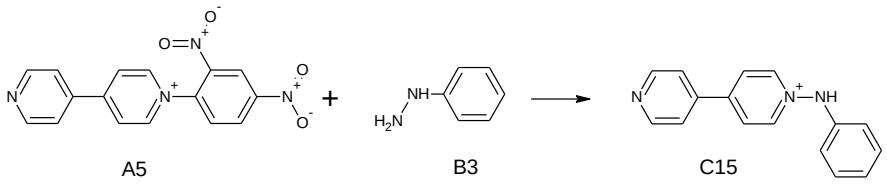

Table 13. Summary table of reaction between A5 and B3.

	A5	**B3**	**C15**
Monoisotopic mass [Da]	323.08	109.08	248.12
Detected [*m/z*]	323	109	248
Retention time R_t [min]	1.3	Dead time	Dead time
Conversion in ES (%)	-	-	ND*
Conversion in bulk (%)	-	-	ND*

* Due to overlapping of peaks in UV-chromatogram, conversion could not be assessed. Reaction had occurred in both ES and bulk.

All results are summarised in Table 14. Reaction conversions for five reactions that occurred in both environment are marked in blue and green rectangles for ES and bulk reactions, respectively. For three reactions where product was observed for ES reaction but not for bulk

reaction, only blue rectangle with conversion is marked. Reactions, where product formation was not observed are marked as “No reaction”. Reactions that were not tested within the scope of this work are marked as “Not done”.

Table 14. Summary of conducted reactions ES and bulk reactions

	B1 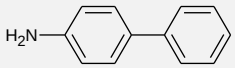 365 nm	B2 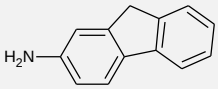 365 nm	B3 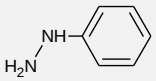
A1 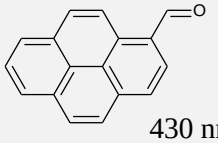 430 nm	Not done	No reaction	4% 9%
A2 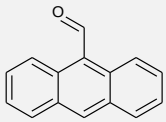 460 nm	No reaction	Not done	12-39%
A3 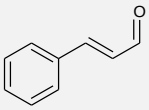	No reaction	Not done	7% ND
A4 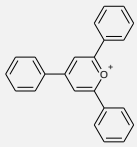 460 nm	ND	24%	Not done
A5 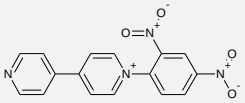	1-5% 9-22%	2-24% 14-58%	ND ND

Bulk ES

4.2. Fluorescence Measurements of Reactions

In order to perform on-line kinetics measurements using laser-induced fluorescence, it is required that one of the reagents and the product are fluorescent and emit light on significantly different wavelengths so that the peaks are differentiable. Reagents chosen for this work are fluorescent and/or potentially increase the conjugated system of the most probable product. It is of importance to assess the conversion of reaction in charged droplets as that indicates whether the reaction can be profiled with LIF. If the reaction occurs too fast/slow, differences in emission spectra cannot be observed.

For reactions where product formation was observed, emission spectra were measured of approximately 2000x diluted ES and bulk solutions. Two Zincke reactions met the requirements of having large difference in emission spectra maxima of reagent and product. The product C13 of reaction between A5 (no emission) and B1 (emission maximum at 365 nm) had the emission peak maximum at 530 nm (Fig. 14). Similarly, the product C14 of Zincke reaction with B2 (emission maximum at 365 nm) had emission spectrum maximum at 565 nm. For confirmation, the product C13 of A5 and B1 reaction was synthesized (purity of 75 wt% based on NMR measurement) and its emission spectrum matched with previous measurements. NMR and emission spectra of the product C13 can be found in SI 3. Additionally, the emission spectrum of ES reaction of 1-pyrenecarboxaldehyde (A1) and phenylhydrazine (B3) had two new peaks proposing more than one fluorescent product or a more complex emission spectrum of the product. In scope of this work, the origin of the peaks was not investigated. Other products did not have fluorescent properties or their emission spectrum maximum overlapped with the one of reagents which made them not suitable for laser probing. Measured fluorescence spectra of fluorescent reagents and reaction mixtures can be found in SI 5.

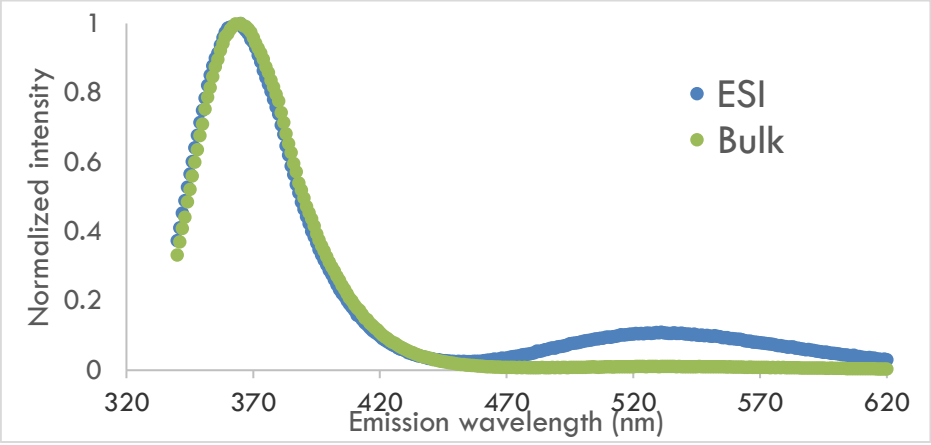

Figure 14. Emission spectra of ES and bulk Zincke reactions between A5 and B1.

4.3. Reaction Kinetics in Bulk Reaction

Reaction kinetics were monitored in bulk for two Zincke reaction between A5 (1-(2,4-dinitrophenyl)-4-(pyridine-4-yl)pyridinium chloride) with B1 (4-aminobiphenyl) and B2 (2-aminofluorene), respectively. Preliminary results of reaction between A5 and B1 did not yield enough data to make conclusions of reaction kinetics. Therefore, reaction between A5 and B2 was selected to perform experiments to obtain information about reaction kinetics parameters. Fluorescence measurements were performed with FluoroMax-4 fluorescence spectrometer and results were cross-checked against kinetics measurements performed by ^{1}H NMR.

4.3.1. Monitoring Bulk Kinetics with Fluorescence Spectroscopy

For fluorescence measurements two solutions with different concentrations were prepared for both reagents, the concentrations can be found in Table 15. Reaction was performed three times and the concentrations were altered from 20 to 57 mM. To carry out reaction, 500 µL of both reagent solutions were pipetted together at room temperature and magnetic stirrer with 250 rpm was used. At time points 60, 120, 180, 240, 300 and 600 s, 10 µl of reaction mixture was pipetted to a separate vial with 2 mL of EtOH (200x dilution) to significantly reduce the reaction rate, effectively stopping the reaction. To measure emission spectra, additional 10x dilutions in EtOH were done to prepare samples suitable for fluorescence measurements. Emission for B2 (2-aminofluorene) was taken as intensity of emission at 365 nm and for the product C14 at 535 nm. Samples were excited at 330 nm and emission spectra were acquired from 350 to 650 nm. The measurements were conducted within the same day.

Assuming that the sum of moles of reagent and the product is constant (1:1 reaction) and knowing the concentration of reagent, product concentrations for all time points were calculated based on the fraction of product emission peak maximum of the sum of emission peaks maxima of B2 and C14 (Fig 15). As fluorescence spectroscopy requires relatively low concentrations and may result high variation in signal intensities caused by inaccuracy of dilution, the fluorescence signal of the product is calibrated by using reagent's signal. Linearity of data points was confirmed and initial reaction rates (slopes) were calculated (Table 16.).

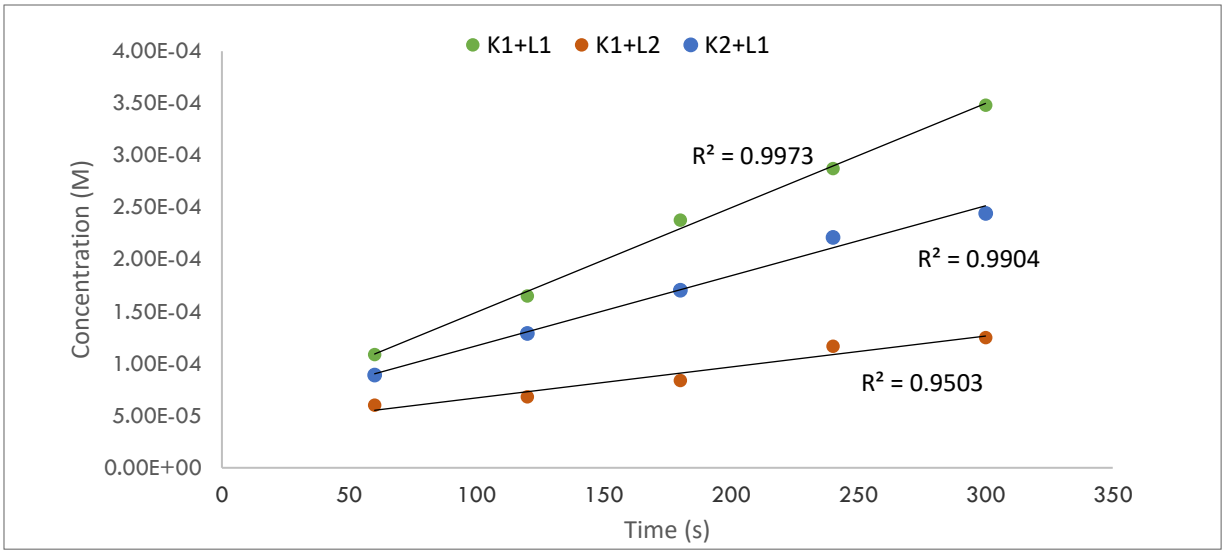

Figure 15. Product C14 formation in time calculated from the fraction of emission spectra maxima of product relative to initial concentration of 2-aminofluorene (B2).

4.3.2. Measuring Kinetics with NMR Spectroscopy

For NMR measurements, reagent solutions of both substances were prepared in deuterated methanol. The substances were first measured separately in NMR (SI) and were then poured together (reaction start time was marked down). NMR spectra were acquired at time with approx. 5 min time intervals. Signals of B2 and product C14 were integrated in respect to the solvent signal assuming the solvent signal to be constant. Linear regression model was fitted to describe the formation of C14 and decrease of B2 (Fig 16).

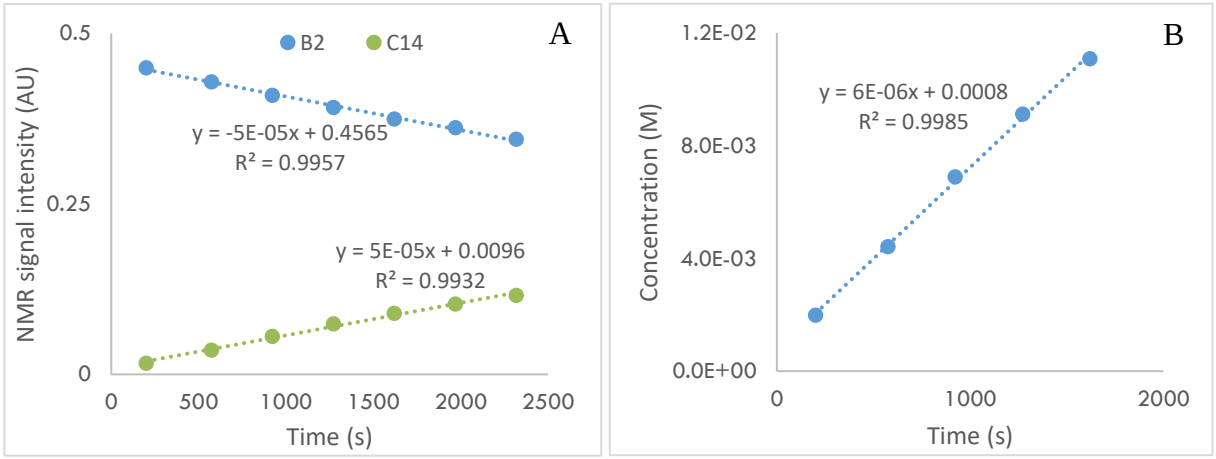

Figure 16. Reaction kinetics monitoring with NMR: A) NMR signals of B2 (2-aminofluorene) decomposition and product C14 formation over time (normalised in respect to solvent); B) Product formation over time, calculated by fraction of product signal in respect to prepared reagent solution concentration of B2.

Table 15. Reagent solutions used in kinetics experiments.

Name	Substance	Concentration [M]	Solvent
S(NMR1)	A5	0.041641	CD_3OD
S(NMR2)	B2	0.05743	CD_3OD
S(K1)	A5	0.041912	EtOH
S(K2)	A5	0.02028	EtOH
S(L1)	B2	0.05246	EtOH
S(L2)	B2	0.027611	EtOH

Table 16. Concentrations used and the initial rates calculated from the experiments.

Experiment	[A5] [M]	[B2] [M]	Initial rate [M/s]
K1 + L1	0.041912	0.05246	1.01E-06
K1 + L2	0.041912	0.027611	3.09E-07
K2 + L1	0.02028	0.05246	7.31E-07
NMR1 + NMR2	0.041641	0.05743	6.7E-06

4.3.3. Results of Kinetics Measurements

Both fluorescence and NMR measurements were confirmed to be suitable for monitoring kinetics for Zincke reaction in bulk between A5 and B2 as linear regression model could be used to describe product formation and initial rates could be obtained.

In NMR measurements it is possible to compare concentrations of reagent and product directly as this method does not require any substance specific corrections. As the slopes for C14 formation and decrease of B2 are approx. same with opposite signs, this method is more accurate for direct measurement of kinetic constant. However, it needs deuterated solvents and cannot be used for in situ reaction monitoring of charged droplets, therefore, fluorescence monitoring of bulk reaction is more beneficial to keep physical parameters similar to droplet reactions.

In fluorescence measurements the signal intensity is dependent on molar extinction coefficient and fluorescence quantum yield of the substance. Therefore, it is important to determine the fluorescence parameters for substances on the specific wavelengths used to assess the kinetic parameters of the reaction. In scope of this work, the product was not synthesised to evaluate its fluorescence properties.

However, reaction orders in respect for reactants can still be calculated based on fluorescence measurements. Reaction orders obtained in this work were 1.85 and 0.45 for B2 and A5 respectively. The overall reaction order for the reaction obtained is 2.30.

Using reaction orders calculated from fluorescence measurements, kinetic constant of k = 0.005587 $M^{-1.30}$ s^{-1} was obtained from NMR kinetics measurement. It is important to note that the NMR experiment was conducted in deuterated solvent which could possibly affect the reaction kinetics and provided kinetic constant may not be equal to kinetic constants measured in other solvents. Although, fractional reaction orders are possible to obtain, they usually indicate more complex reaction mechanisms and integer reaction order for simple reactions are more common. Considering that experimental results are presented without replicas and deviation is difficult to assess, rate law of second-order reaction could be good approximation for bimolecular reaction.

To confirm the kinetics measurements with fluorescence spectroscopy and apply corrections, synthesis of product and determination of fluorescence parameters need to be performed. Therefore, these results prove the possibility to measure kinetics with fluorescence spectrometry and are a good basis for first assessments yet need further confirmation and corrections.

4.4. Further Prospects

To perform laser induced fluorescence measurements, the reagents for two Zincke reactions (1-(2,4-dinitrophenyl)-4-(pyridine-4-yl)pyridinium chloride (A5) reaction with 2-aminofluorene (B2) and 4-aminobiphenyl (B1) respectively) have been sent to Federal Institute for Materials Research and Testing (BAM) in Berlin, Germany. Our collaborators have the capability to build suitable experiment setup for characterization of electrospray and use single-expose LIF photography to acquire fluorescence emission spectra of the spray, which provides possibility to obtain additional information of droplet size-distribution and velocity range.[42]

In order to directly compare kinetics in bulk and charged droplets with fluorescence spectroscopy, product should be synthesised and additional experiments to determine molar extinction coefficients must be conducted on the same excitation wavelength that is used for monitoring reaction kinetics in both bulk and droplets. The preliminary kinetics monitoring of the Zincke reaction was carried out, yet results should be confirmed with additional measurements.

Conclusion

Charged droplets are promising environment to carry out reactions on accelerated rates and potentially reduce the use of catalysts and solvents. Number of reactions have been shown to occur with higher reaction rates and without the use of catalyst. The reaction rates are predominantly calculated by knowing the distance between the needle and the counter electrode, however, in situ reaction monitoring has not been conducted. In scope of this work, suitable reactions for in situ reaction kinetics monitoring were determined for further investigation with laser induced fluorescence spectroscopy. For that, fluorescence emission of one reagent and product on different wavelengths is required.

Four types of reactions – imine/hydrazone formation, Katritzky and Zincke reactions were tested in charged droplets and conformational bulk reactions were conducted. Conversion was assessed based on LC-MS analysis and fluorescence spectroscopy was used to measure emission spectra of reaction mixtures.

The most successful reactions investigated in this work were two Zincke reactions that occurred in both bulk and charged droplets, with accelerated rates in the latter. For both, the product had a different emission spectrum maximum compared to reagent (565 and 530 nm for products of Zincke reactions with 2-aminofluorene (B2, 365 nm) and 4-aminobiphenyl (B1, 365 nm), respectively). These reactions were found suitable for spray probing with laser induced fluorescence and the collaboration with Federal Institute for Materials Research and Testing (BAM) in Berlin, Germany is ongoing.

Hydrazone formation and Katritzky reactions were similarly successful based on LC-MS analysis, however, the measured emission spectra indicated that the formed product was not fluorescent for most of the cases. The product C3 of 1-pyrenecarboxaldehyde (A1) and phenylhydrazine (B3) produced more complex emission spectra which was not further investigated in scope of this work.

LC-MS analysis for imine formation reactions indicated no product formation. However, hydrazone formation that occurs in the same manner was successful implying that produced imines might have been less stable and hydrolysed in LC system during analysis.

The reaction kinetics in bulk reaction were investigated for Zincke reaction between 1-(2,4-dinitrophenyl)-4-(pyridine-4-yl)pyridinium chloride (A5) and 2-aminofluorene (B2) to confirm the suitability of fluorescence spectroscopy for reaction monitoring in charged droplets. The

initial rates method was proven to be successful to monitor kinetics in bulk. Reaction orders of 1.85 and 0.45 were obtained for substances B2 and A5, respectively. Overall reaction order 2.30 and kinetic constant k = 0.005587 $M^{-1.303}s^{-1}$ were obtained for the reaction. However, the product needs to be synthesised and molar extinction coefficients need to be determined on the specific wavelength for reagent and product in order to verify kinetic constant.

The in-house built spray system was proven to be successful to accelerate reactions. Suitable reactions for monitoring reaction kinetics in electrospray were detected and further research is ongoing to elucidate reaction kinetics and mechanisms in charged droplets.

References

(1) Dobson, C. M.; Ellison, G. B.; Tuck, A. F.; Vaida, V. Atmospheric Aerosols as Prebiotic Chemical Reactors. *Proceedings of the National Academy of Sciences* **2000**, *97* (22), 11864–11868. https://doi.org/10.1073/pnas.200366897.

(2) Holmberg, K. Organic Reactions in Microemulsions. *European Journal of Organic Chemistry* **2007**, *5*, 731–742. https://doi.org/10.1002/ejoc.200600741.

(3) Crawford, E. A.; Esen, C.; Volmer, D. A. Real Time Monitoring of Containerless Microreactions in Acoustically Levitated Droplets via Ambient Ionization Mass Spectrometry. *Analytical Chemistry* **2016**, *88* (17), 8396–8403. https://doi.org/10.1021/acs.analchem.6b01519.

(4) Bain, R. M.; Pulliam, C. J.; Thery, F.; Cooks, R. G. Accelerated Chemical Reactions and Organic Synthesis in Leidenfrost Droplets. *Angewandte Chemie International Edition* **2016**, *55* (35), 10478–10482. https://doi.org/10.1002/anie.201605899.

(5) Fedick, P. W.; Iyer, K.; Wei, Z.; Avramova, L.; Capek, G. O.; Cooks, R. G. Screening of the Suzuki Cross-Coupling Reaction Using Desorption Electrospray Ionization in High-Throughput and in Leidenfrost Droplet Experiments. *Journal of The American Society for Mass Spectrometry* **2019**, *30* (10), 2144–2151. https://doi.org/10.1007/s13361-019-02287-3.

(6) Badu-Tawiah, A. K.; Campbell, D. I.; Cooks, R. G. Accelerated C–N Bond Formation in Dropcast Thin Films on Ambient Surfaces. *Journal of The American Society for Mass Spectrometry* **2012**, *23* (9), 1461–1468. https://doi.org/10.1007/s13361-012-0394-y.

(7) Li, Y.; Yan, X.; Cooks, R. G. The Role of the Interface in Thin Film and Droplet Accelerated Reactions Studied by Competitive Substituent Effects. *Angew. Chem. Int. Ed.* **2016**, *55* (10), 3433–3437. https://doi.org/10.1002/anie.201511352.

(8) Yan, X.; Cheng, H.; Zare, R. N. Two-Phase Reactions in Microdroplets without the Use of Phase-Transfer Catalysts. *Angewandte Chemie International Edition* **2017**, *56* (13), 3562–3565. https://doi.org/10.1002/anie.201612308.

(9) La Sorella, G.; Strukul, G.; Scarso, A. Recent Advances in Catalysis in Micellar Media. *Green Chemistry* **2015**, *17* (2), 644–683. https://doi.org/10.1039/C4GC01368A.

(10) Yan, X.; Bain, R. M.; Cooks, R. G. Organic Reactions in Microdroplets: Reaction Acceleration Revealed by Mass Spectrometry. *Angewandte Chemie International Edition* **2016**, *55* (42), 12960–12972. https://doi.org/10.1002/anie.201602270.

(11) Banerjee, S.; Zare, R. N. Syntheses of Isoquinoline and Substituted Quinolines in Charged Microdroplets. *Angewandte Chemie International Edition* **2015**, *54* (49), 14795–14799. https://doi.org/10.1002/anie.201507805.

(12) Fallah-Araghi, A.; Meguellati, K.; Baret, J.-C.; Harrak, A. E.; Mangeat, T.; Karplus, M.; Ladame, S.; Marques, C. M.; Griffiths, A. D. Enhanced Chemical Synthesis at Soft Interfaces: A Universal Reaction-Adsorption Mechanism in Microcompartments. *Physical Review Letters* **2014**, *112* (2). https://doi.org/10.1103/PhysRevLett.112.028301.

(13) Cech, N. B.; Enke, C. G. Practical Implications of Some Recent Studies in Electrospray Ionization Fundamentals. *Mass Spectrom. Rev.* **2001**, *20* (6), 362–387. https://doi.org/10.1002/mas.10008.

(14) Konermann, L.; Ahadi, E.; Rodriguez, A. D.; Vahidi, S. Unraveling the Mechanism of Electrospray Ionization. *Anal. Chem.* **2013**, *85* (1), 2–9. https://doi.org/10.1021/ac302789c.

(15) Bain, R. M.; Ayrton, S. T.; Cooks, R. G. Fischer Indole Synthesis in the Gas Phase, the Solution Phase, and at the Electrospray Droplet Interface. *Journal of The American Society for Mass Spectrometry* **2017**, *28* (7), 1359–1364. https://doi.org/10.1007/s13361-017-1597-z.

(16) Bain, R. M.; Pulliam, C. J.; Yan, X.; Moore, K. F.; Müller, T.; Cooks, R. G. Mass Spectrometry in Organic Synthesis: Claisen–Schmidt Base-Catalyzed Condensation and Hammett Correlation of Substituent Effects. *Journal of Chemical Education* **2014**, *91* (11), 1985–1989. https://doi.org/10.1021/ed500288m.

(17) Bain, R. M.; Sathyamoorthi, S.; Zare, R. N. "On-Droplet" Chemistry: The Cycloaddition of Diethyl Azodicarboxylate and Quadricyclane. *Angewandte Chemie International Edition* **2017**, *56* (47), 15083–15087. https://doi.org/10.1002/anie.201708413.

(18) Yan, X.; Augusti, R.; Li, X.; Cooks, R. G. Chemical Reactivity Assessment Using Reactive Paper Spray Ionization Mass Spectrometry: The Katritzky Reaction. *ChemPlusChem* **2013**, *78* (9), 1142–1148. https://doi.org/10.1002/cplu.201300172.

(19) Fedick, P. W.; Bain, R. M.; Bain, K.; Mehari, T. F.; Cooks, R. G. Accelerated Tert - Butyloxycarbonyl Deprotection of Amines in Microdroplets Produced by a Pneumatic Spray. *International Journal of Mass Spectrometry* **2018**, *430*, 98–103. https://doi.org/10.1016/j.ijms.2018.05.009.

(20) Nam, I.; Nam, H. G.; Zare, R. N. Abiotic Synthesis of Purine and Pyrimidine Ribonucleosides in Aqueous Microdroplets. *Proceedings of the National Academy of Sciences* **2018**, *115* (1), 36–40. https://doi.org/10.1073/pnas.1718559115.s

(21) Nam, I.; Lee, J. K.; Nam, H. G.; Zare, R. N. Abiotic Production of Sugar Phosphates and Uridine Ribonucleoside in Aqueous Microdroplets. *Proceedings of the National Academy of Sciences* **2017**, *114* (47), 12396–12400. https://doi.org/10.1073/pnas.1714896114.

(22) Bain, R. M.; Pulliam, C. J.; Cooks, R. G. Accelerated Hantzsch Electrospray Synthesis with Temporal Control of Reaction Intermediates. *Chemical Science* **2015**, *6* (1), 397–401. https://doi.org/10.1039/C4SC02436B.

(23) Sahota, N.; AbuSalim, D. I.; Wang, M. L.; Brown, C. J.; Zhang, Z.; El-Baba, T. J.; Cook, S. P.; Clemmer, D. E. A Microdroplet-Accelerated Biginelli Reaction: Mechanisms and Separation of Isomers Using IMS-MS. *Chem. Sci.* **2019**, *10* (18), 4822–4827. https://doi.org/10.1039/C9SC00704K.

(24) Berkel, G. J. V.; Asano, K. G.; Schnier, P. D. Electrochemical Processes in a Wire-in-a-Capillary Bulk-Loaded, Nano-Electrospray Emitter. *J Am Soc Mass Spectrom* **2001**, 10.

(25) Banerjee, S. Induction of Protein Conformational Change inside the Charged Electrospray Droplet. *J. Mass Spectrom.* **2013**, 13.

(26) Girod, M.; Moyano, E.; Campbell, D. I.; Cooks, R. G. Accelerated Bimolecular Reactions in Microdroplets Studied by Desorption Electrospray Ionization Mass Spectrometry. *Chem. Sci.* **2011**, *2* (3), 501–510. https://doi.org/10.1039/C0SC00416B.

(27) Rovelli, G.; Jacobs, M. I.; Willis, M. D.; Rapf, R. J.; Prophet, A. M.; Wilson, K. R. A Critical Analysis of Electrospray Techniques for the Determination of Accelerated Rates and Mechanisms of Chemical Reactions in Droplets. *Chem. Sci.* **2020**, *11* (48), 13026–13043. https://doi.org/10.1039/D0SC04611F.

(28) Lee, J. K.; Banerjee, S.; Nam, H. G.; Zare, R. N. Acceleration of Reaction in Charged Microdroplets. *Quarterly Reviews of Biophysics* **2015**, *48* (04), 437–444. https://doi.org/10.1017/S0033583515000086.

(29) Xie, J.; Jiang, J.; Davoodi, P.; Srinivasan, M. P.; Wang, C.-H. Electrohydrodynamic Atomization: A Two-Decade Effort to Produce and Process Micro-/Nanoparticulate Materials. *Chemical Engineering Science* **2015**, *125*, 32–57. https://doi.org/10.1016/j.ces.2014.08.061.

(30) Fantini, D.; Zanetti, M.; Costa, L. Polystyrene Microspheres and Nanospheres Produced by Electrospray. *Macromolecular Rapid Communications* **2006**, *27* (23), 2038–2042. https://doi.org/10.1002/marc.200600532.

(31) Ikeuchi, M.; Tane, R.; Ikuta, K. Electrospray Deposition and Direct Patterning of Polylactic Acid Nanofibrous Microcapsules for Tissue Engineering. *Biomed Microdevices* **2012**, *14* (1), 35–43. https://doi.org/10.1007/s10544-011-9583-x.

(32) Li, Y.; Liu, Y.; Gao, H.; Helmy, R.; Wuelfing, W. P.; Welch, C. J.; Cooks, R. G. Accelerated Forced Degradation of Pharmaceuticals in Levitated Microdroplet Reactors. *Chem. Eur. J.* **2018**, 5.

(33) Wei, Z.; Li, Y.; Cooks, R. G.; Yan, X. Accelerated Reaction Kinetics in Microdroplets: Overview and Recent Developments. *Annu. Rev. Phys. Chem.* **2020**, *71* (1), 31–51. https://doi.org/10.1146/annurev-physchem-121319-110654.

(34) Telle, H. H.; González Ureña, A.; Donovan, R. J. *Laser Chemistry: Spectroscopy, Dynamics and Applications*; John Wiley & Sons: Chichester, West Sussex, England ; Hoboken, NJ, 2007.

(35) Zhou, S.; Edwards, A. G.; Cook, K. D.; Van Berkel, G. J. Investigation of the Electrospray Plume by Laser-Induced Fluorescence Spectroscopy. *Anal. Chem.* **1999**, *71* (4), 769–776. https://doi.org/10.1021/ac981259r.

(36) Wang, R.; Zenobi, R. Evolution of the Solvent Polarity in an Electrospray Plume. *J Am Soc Mass Spectrom* **2010**, *21* (3), 378–385. https://doi.org/10.1016/j.jasms.2009.10.022.

(37) Gibson, S. C.; Feigerle, C. S.; Cook, K. D. Fluorometric Measurement and Modeling of Droplet Temperature Changes in an Electrospray Plume. *Anal. Chem.* **2014**, *86* (1), 464–472. https://doi.org/10.1021/ac402364g.

(38) Soleilhac, A.; Dagany, X.; Dugourd, P.; Girod, M.; Antoine, R. Correlating Droplet Size with Temperature Changes in Electrospray Source by Optical Methods. *Anal. Chem.* **2015**, *87* (16), 8210–8217. https://doi.org/10.1021/acs.analchem.5b00976.

(39) Hemming, K. Organic Chemistry. By J. P. Clayden, N. Greeves, S. Warren, and P. D. Wothers; Oxford University Press, 2001, ISBN 0 19 850346 6, 53 Chapters, 1508 *Chem. Educator* **2001**, *6* (6), 396–398. https://doi.org/10.1007/s00897010513a.

(40) Smith, M. B.; March, J. *March's Advanced Organic Chemistry*; John Wiley & Sons, Inc.: Hoboken, NJ, USA, 2006. https://doi.org/10.1002/0470084960.

(41) Schoder, S.; Schröder, H. V.; Cera, L.; Puttreddy, R.; Güttler, A.; Resch-Genger, U.; Rissanen, K.; Schalley, C. A. Strong Emission Enhancement in PH-Responsive 2:2 Cucurbit[8]Uril Complexes. *Chem. Eur. J.* **2019**, chem.201806337. https://doi.org/10.1002/chem.201806337.

(42) Stindt, A.; Warschat, C.; Bierstedt, A.; Panne, U.; Riedel, J. Characterisation of An Inexpensive Sonic Spray Ionisation Source Using Laser-Induced Fluorescence Imaging and Mass Spectrometry. *Eur J Mass Spectrom (Chichester)* **2014**, *20* (1), 21–29. https://doi.org/10.1255/ejms.1242.

Supplementary Information

SI 1. Substances Used in This Study

Name	CAS number	M [g/mol]	Emission max [nm]	Structure
1-pyrenecarboxaldehyde	3029-19-4	230.26	430	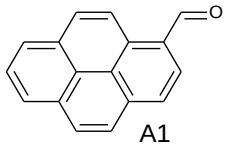 A1
9-anthracenecarboxaldehyde	642-31-9	206.24	460	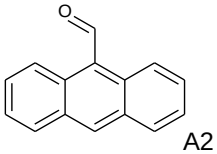 A2
cinnamaldehyde	14371-10-9	132.16	-	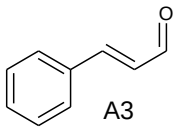 A3
2,4,6-triphenylpyrylium tetrafluoroborate	448-61-3	396.19	460	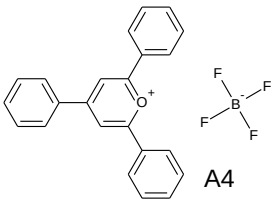 A4
1-(2,4-dinitrophenyl)-4-(pyridine-4-yl)pyridinium chloride	-	358.74	-	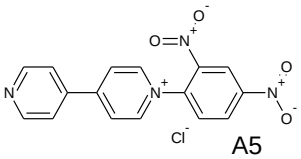 A5
4-aminobiphenyl	92-67-1	169.22	365	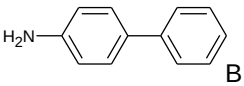 B1
2-aminofluorene	6344-63-4	181.23	365	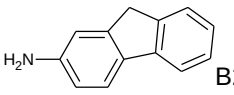 B2
phenylhydrazine	100-63-0	108.14	-	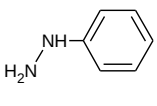 B3

SI 2. Synthesis of 1-(2,4-dinitrophenyl)-4-(pyridine-4-yl)pyridinium chloride (A5)

1.08 g of 4,4'-bipyridine (156.18 g/mol, 6.9 mmol) and 1.54 g 1-chloro-2,4-dinitrobenzene (202.55 g/mol, 7.6 mmol) were weighed into round-bottom flask. 30 mL of acetone was added and the mixture was stirred with magnetic stirrer for 48 h on 70°C. Grey precipitation was washed with hexane and dichloromethane on a filter paper. The product was confirmed with NMR. Further purification was not performed and product containing approx. 3 wt% of 4.4'-bipyridine was used for syntheses.

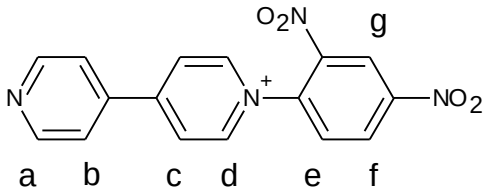

^{1}H NMR (700 MHz, DMSO-d6) δ = 9.43 (d, J = 7.1 Hz, 2H, H_d), 9.30 (d, J = 2.5 Hz, 1H, H_g), 8.95 (dd, J = 8.6, 2.5 Hz, 1H, H_f), 8.90 (dd, J =4.5, 1.8 Hz, 2H, H_c), 8.83 (d, J =7.0 Hz, 2H, H_a), 8.36 (d, J = 8.6 Hz, 1H, H_e), 8.13 (dd, J = 4.5, 1.7 Hz, 2H, H_b) ppm.

SI 2.1. NMR spectrum of 1-(2,4-dinitrophenyl)-4-(pyridine-4-yl)pyridinium chloride (A5)

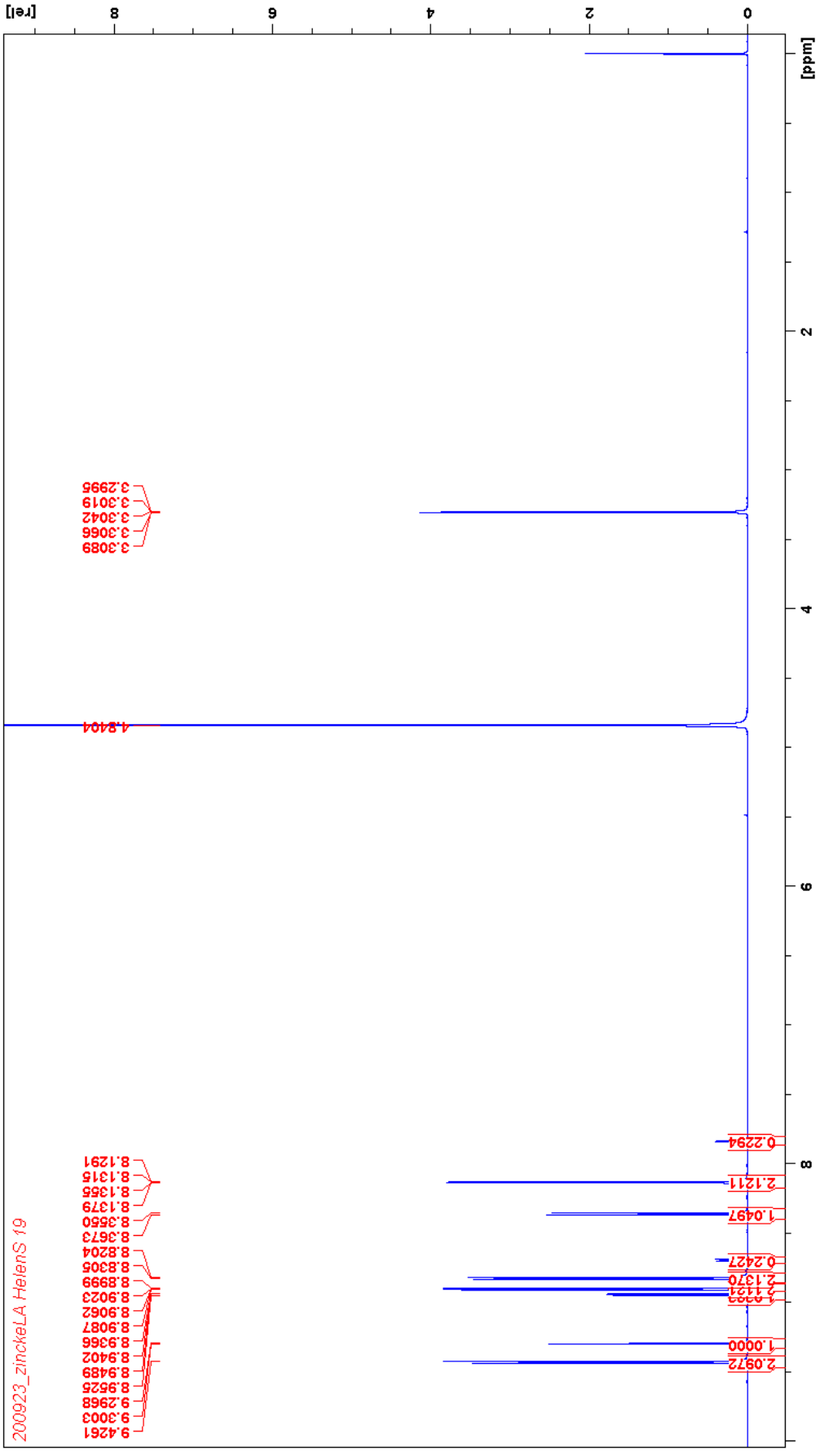

SI 3. NMR and Fluorescence Emission Spectrum of 1-(biphenyl-4-yl)-4-(pyridin-4-yl)pyridinium (C13)

78 mg of x and 94 mg of 4-aminobiphenyl were weighed into round-bottom flask. Reagents were dissolvend in 2 mL EtOH and stirred at 80°C with magnetic stirrer for 48 h. Solvent was evaporated and the precipitation was washed on filter paper with acetone. The product was confirmed with NMR. Further purification was not performed and product containing approx. 25 wt% of 4-aminobiphenyl was obtained.

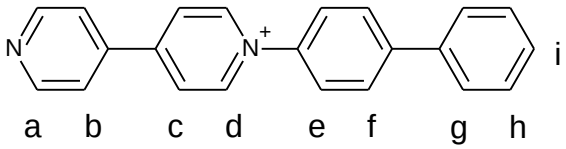

^{1}H NMR (700 MHz, DMSO-d6) δ = 9.59 (d, J = 6.9 Hz, 2H, H_d), 8.92 (d, J = 6.0 Hz, 2H, H_a), 8.84 (d, J = 6.9 Hz, 2H, H_c), 8.19 (d, J = 6.0 Hz, 2H, H_b), 8.07 (m, 4H, H_e & H_f), 7.83 (d, J = 7.3 Hz, 2H, H_g), 7.56 (t, J = 7.6 Hz, 2H, H_h), 7.48 (t, J = 7.4 Hz, 1H, H_i) ppm.

SI 3.1. Fluorescence emission spectrum of 1-(biphenyl-4-yl)-4-(pyridin-4-yl)pyridinium (C13)

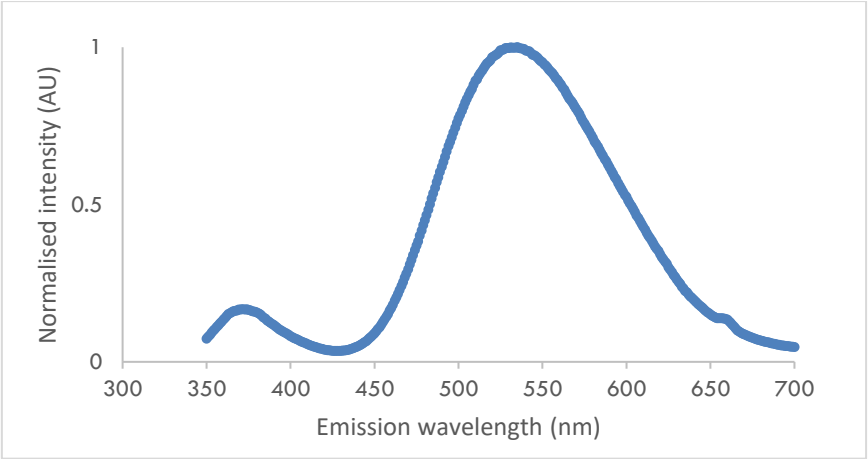

SI 3.2. NMR spectrum of 1-(biphenyl-4-yl)-4-(pyridin-4-yl)pyridinium (C13)

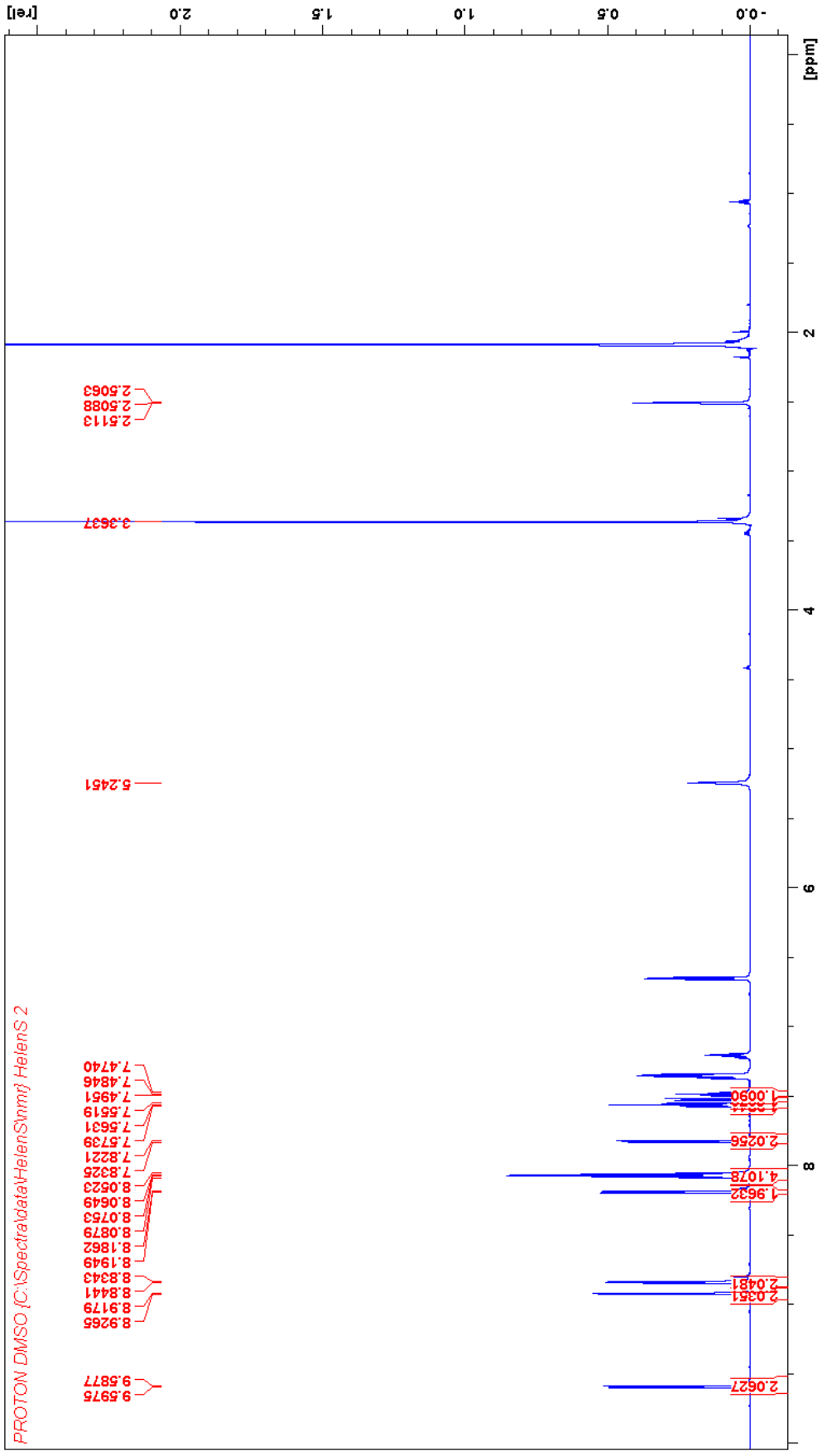

SI 4. LC-MS UV-Chromatograms and Mass Spectra

SI 4.1. 1-Pyrenecarboxaldehyde (A1) + 2-Aminofluorene (B2)

Figure SI 4.1.1. UV-chromatogram (254 nm) of ES reaction of A1 and B2 measured with Agilent QQQ LC system.

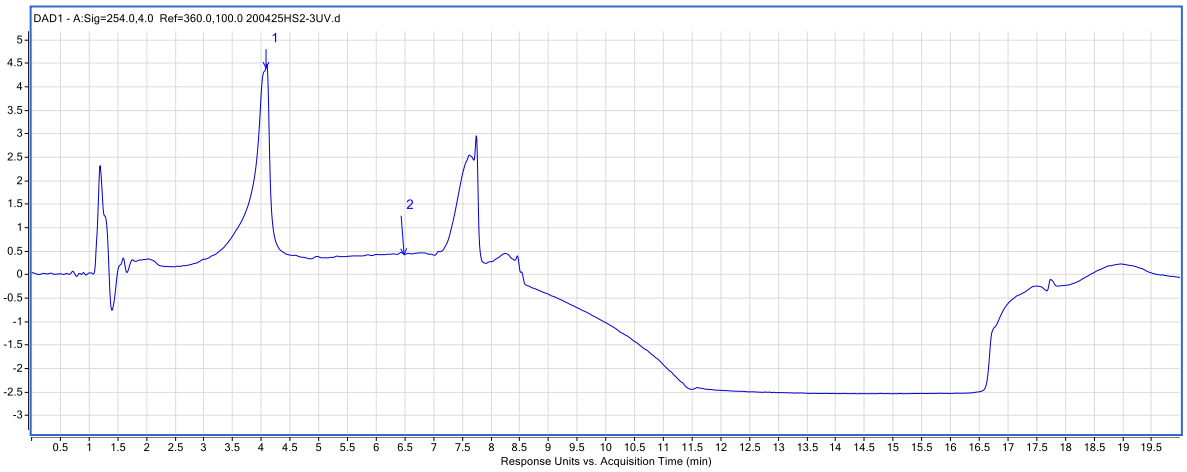

Table SI 4.1.1. Detailed MS data of ES reaction of A1 and B2.

	MS spectrum
1	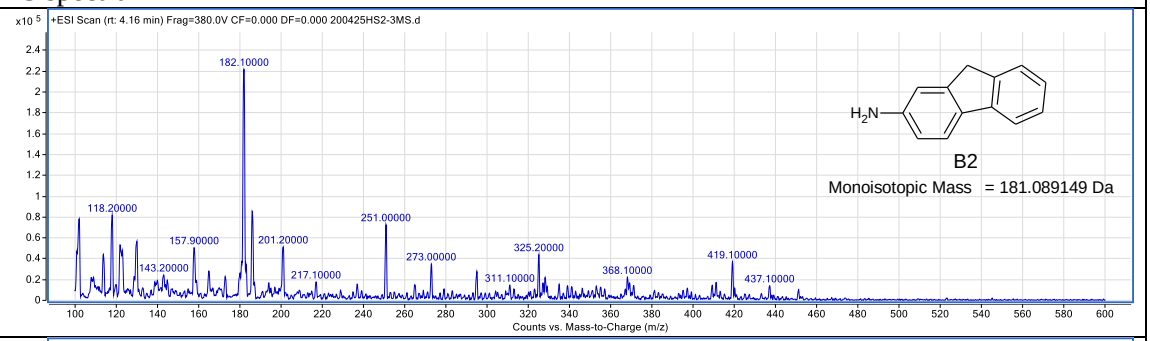
2	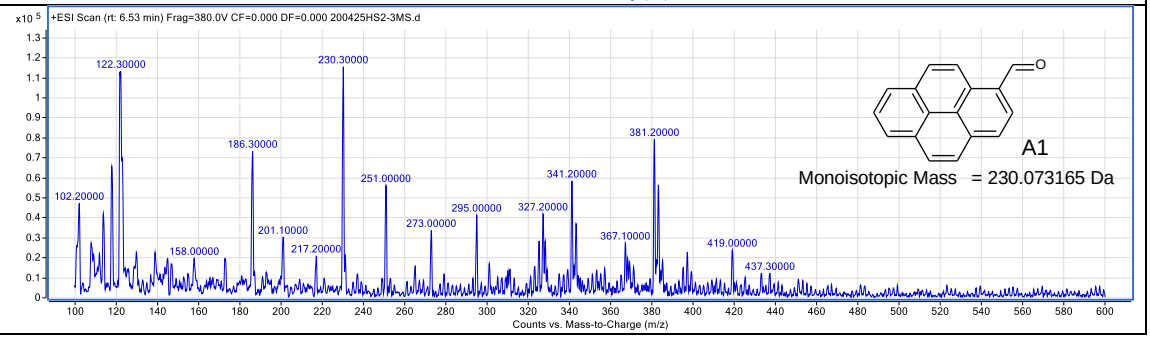

Figure SI 4.1.2. UV-chromatogram (254 nm) of bulk reaction of A1 and B2 measured with Agilent QQQ LC system.

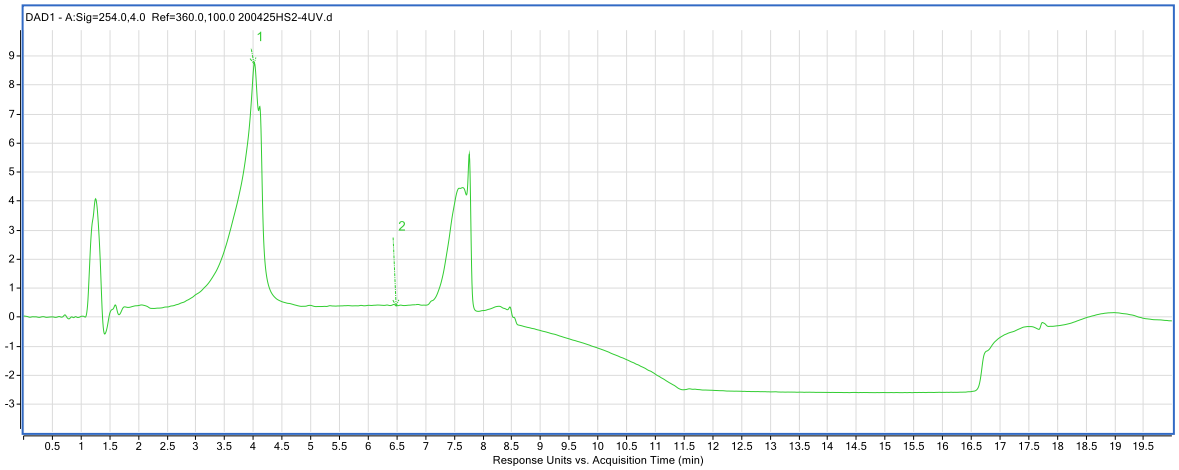

Table SI 4.1.2. Detailed MS data of bulk reaction of A1 and B2.

	MS spectrum
1	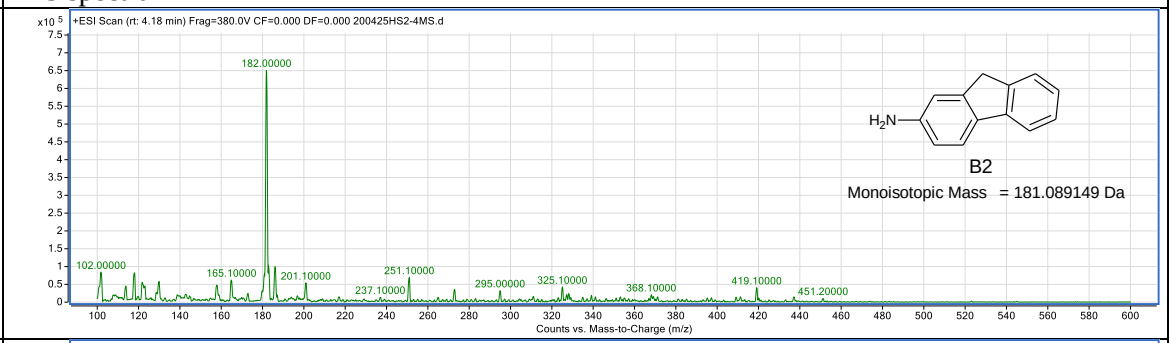
2	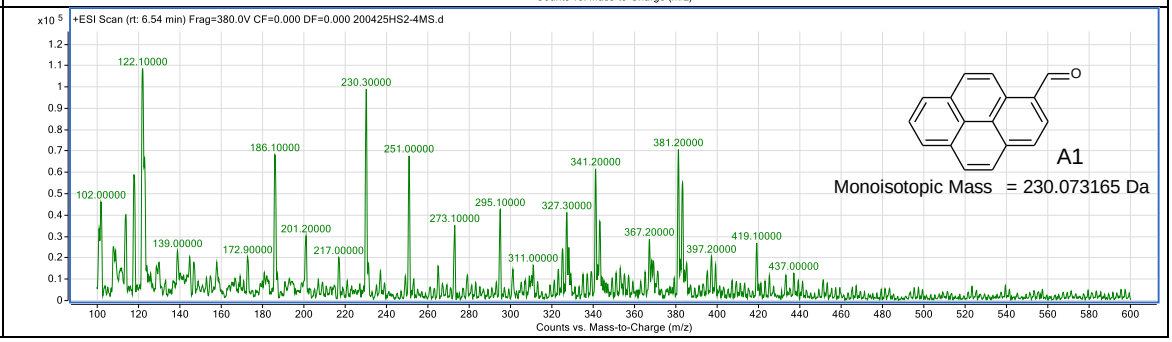

SI 4.2. 1-Pyrenecarboxaldehyde (A1) + Phenylhydrazine (B3)

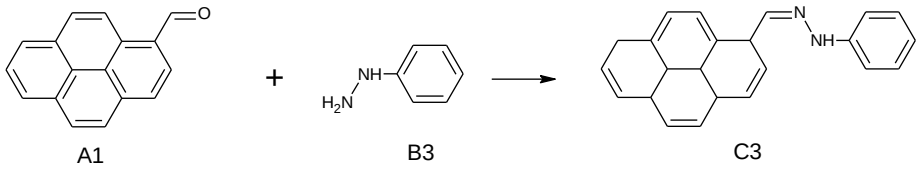

Figure SI 4.2.1. UV-chromatogram (254 nm) of ES reaction of A1 and B3 measured with Agilent XCT LC system.

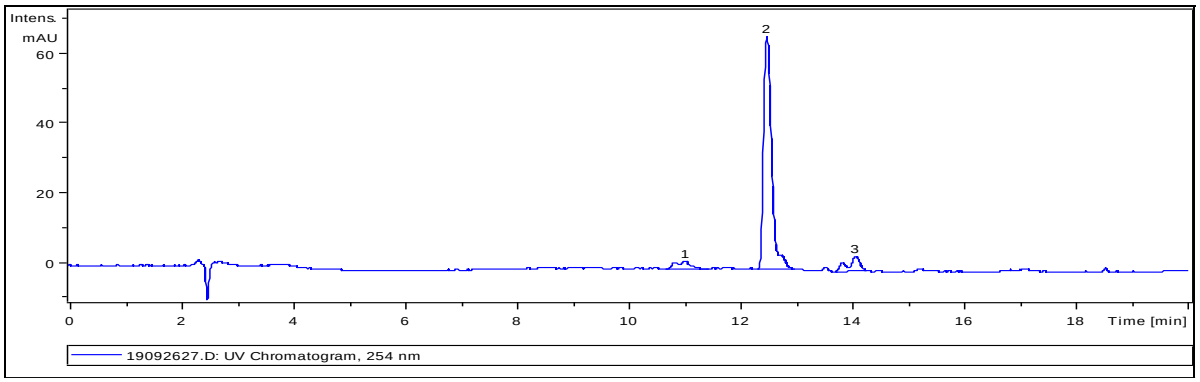

Table SI 4.2.1. Detailed MS data of ES reaction of A1 and B3.

	MS spectrum
1	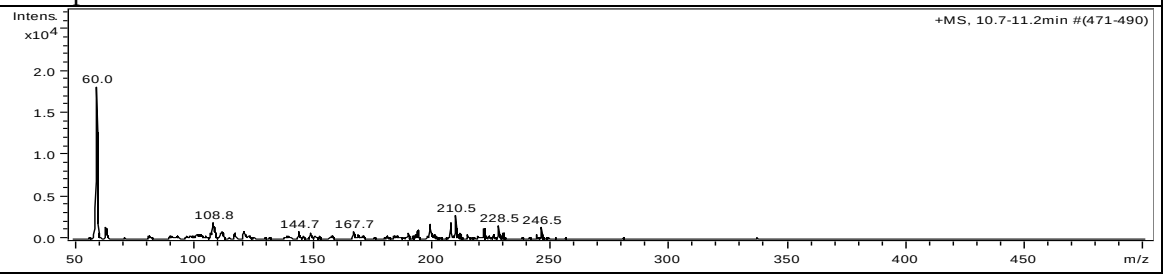
2	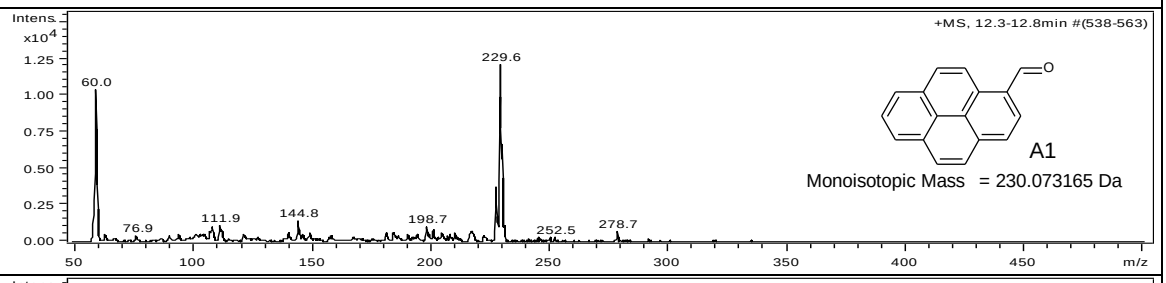
3	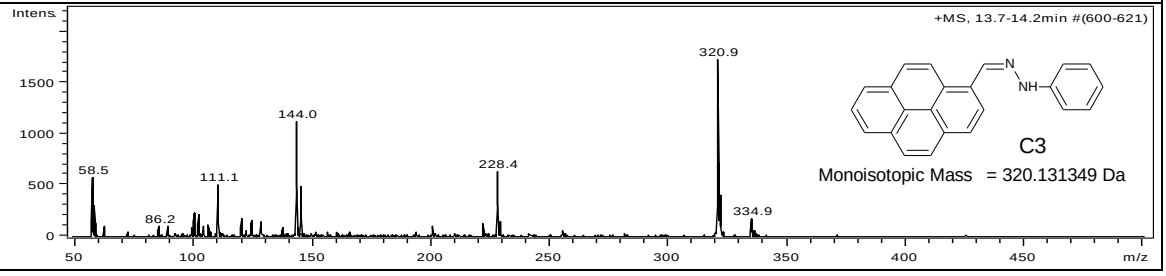

Figure SI 4.2.2. UV-chromatogram (254 nm) of bulk reaction of A1 and B3 measured with Agilent XCT LC system.

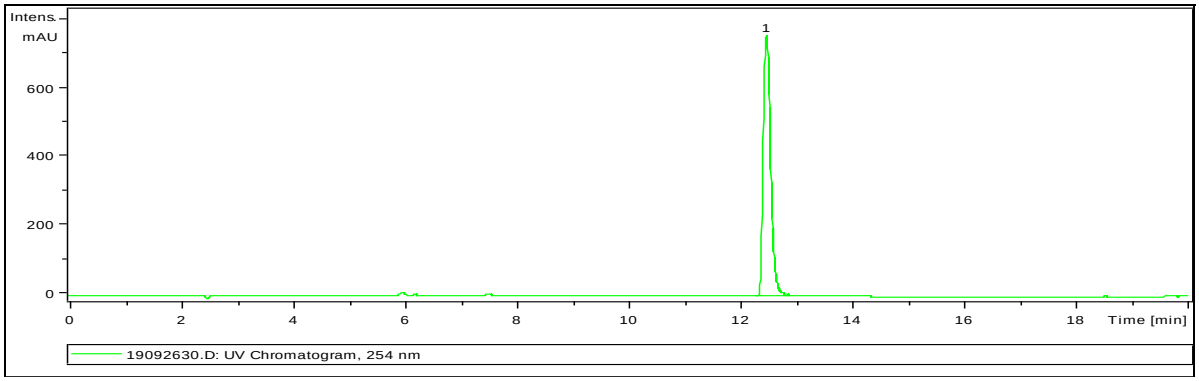

Table SI 4.2.2. Detailed MS data of bulk reaction of A1 and B3.

	MS spectrum
1	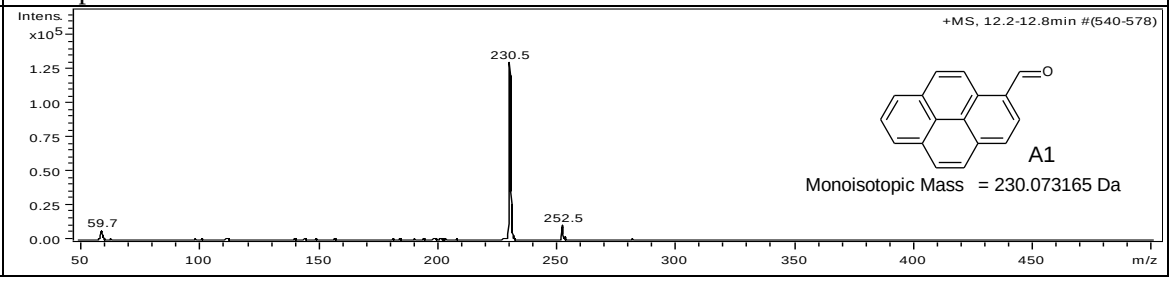

SI 4.3. 9-Anthracenecarboxaldehyde (A2) + 4-Aminobiphenyl (B1)

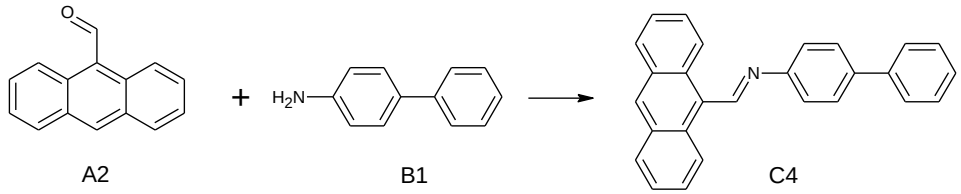

Figure SI 4.3.1. UV-chromatogram (254 nm) of ES reaction of A2 and B1 measured with Agilent XCT LC system.

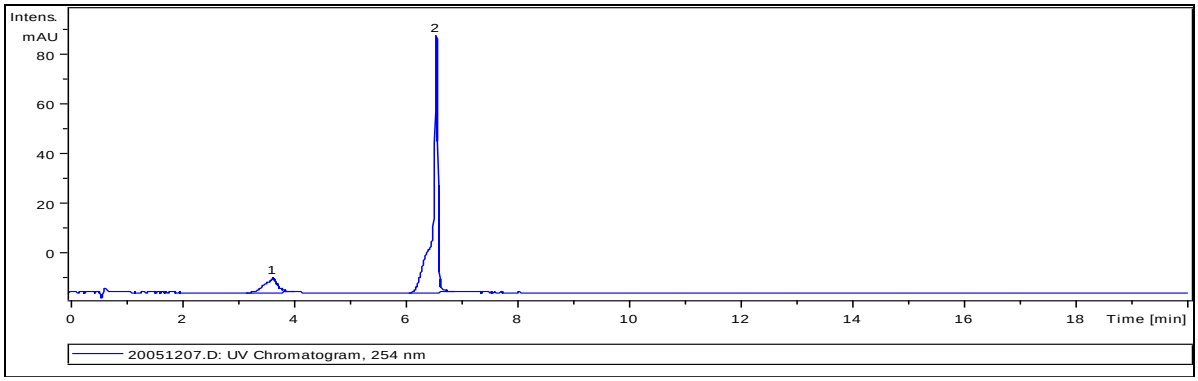

Table SI 4.3.1. Detailed MS data of ES reaction of A2 and B1.

	MS spectrum
1	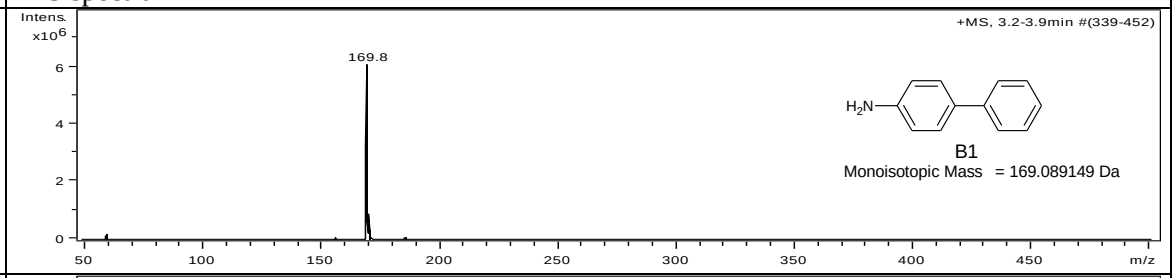
2	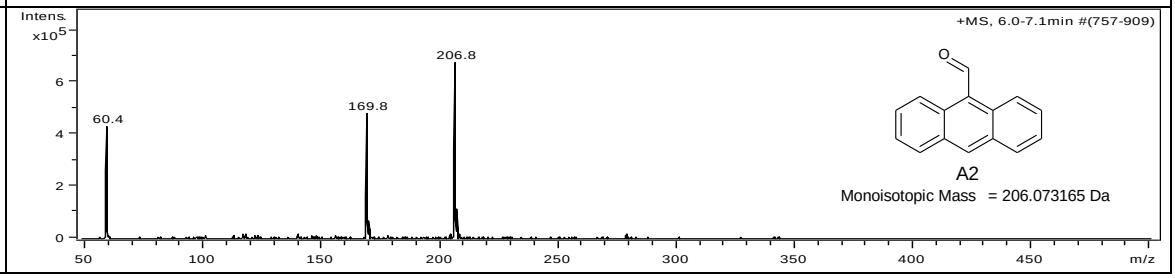

Figure SI 4.3.2. UV-chromatogram (254 nm) of bulk reaction of A2 and B1 measured with Agilent XCT LC system.

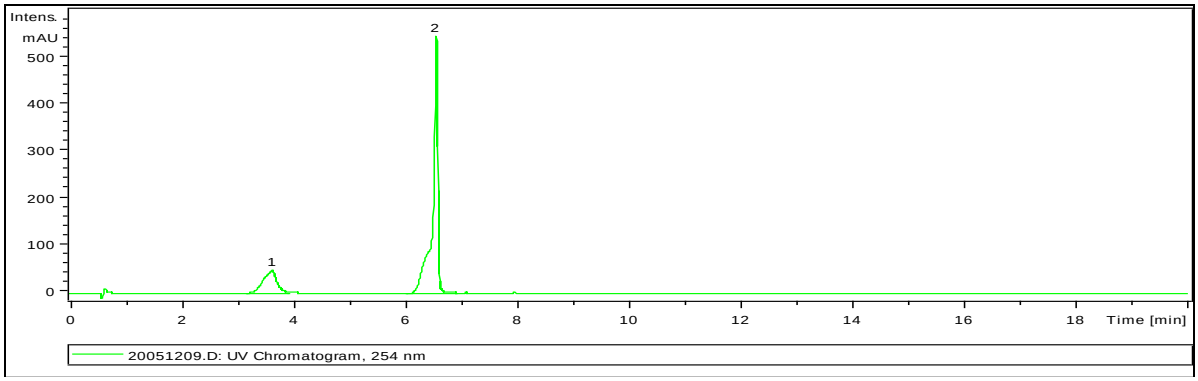

Table SI 4.3.2. Detailed MS data of bulk reaction of A2 and B1.

	MS spectrum
1	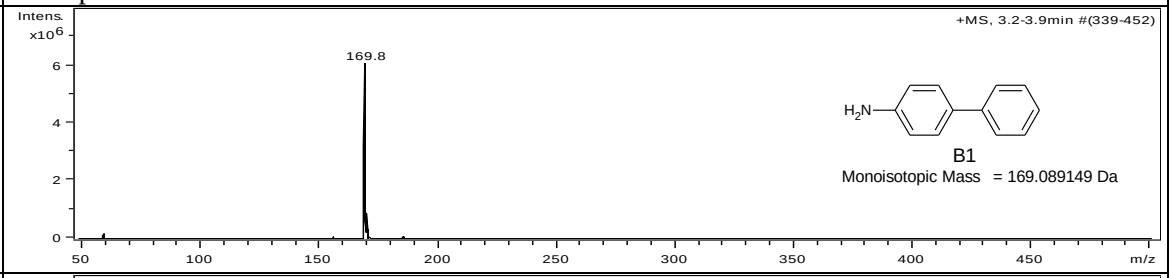
2	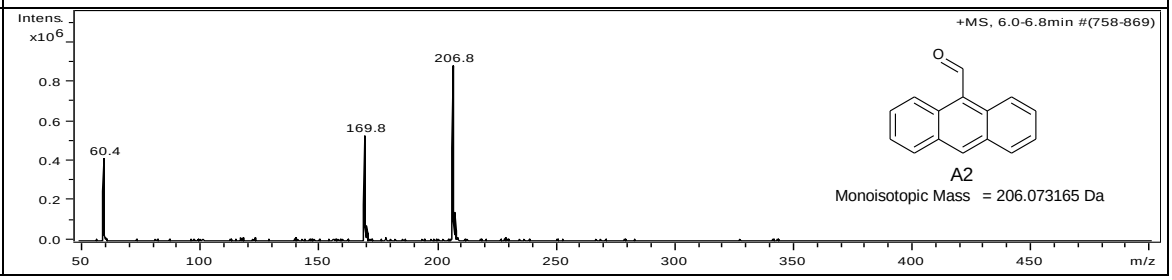

SI 4.4. 9-Anthracenecarboxaldehyde (A2) + Phenylhydrazine (B3)

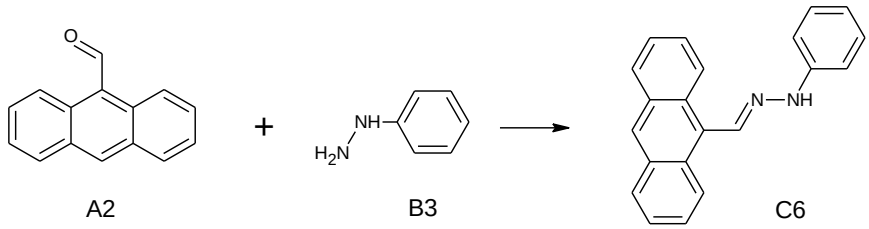

Figure SI 4.4.1. UV-chromatogram (254 nm) of ES reaction of A2 and B3 measured with Agilent XCT LC system.

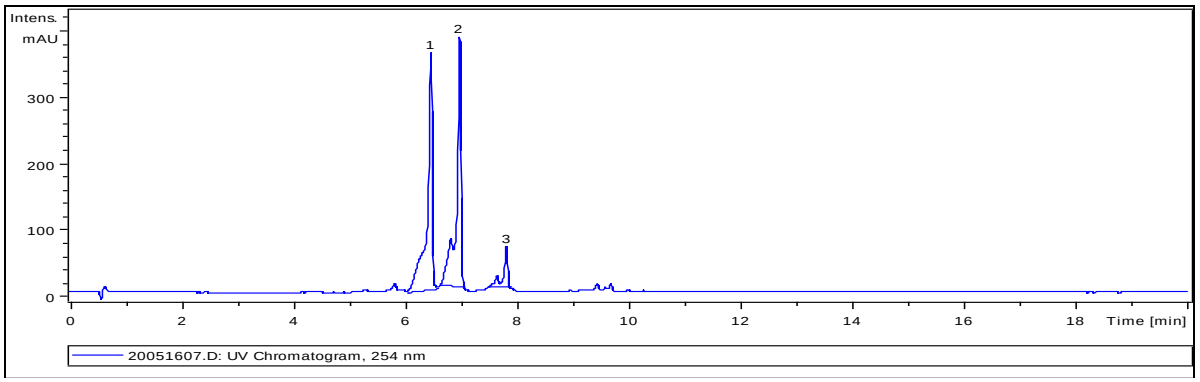

Table SI 4.4.1. Detailed MS data of ES reaction of A2 and B3.

	MS spectrum
1	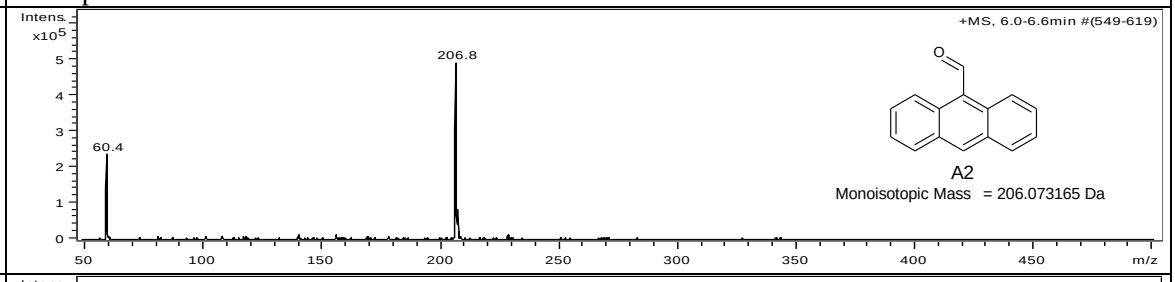
2	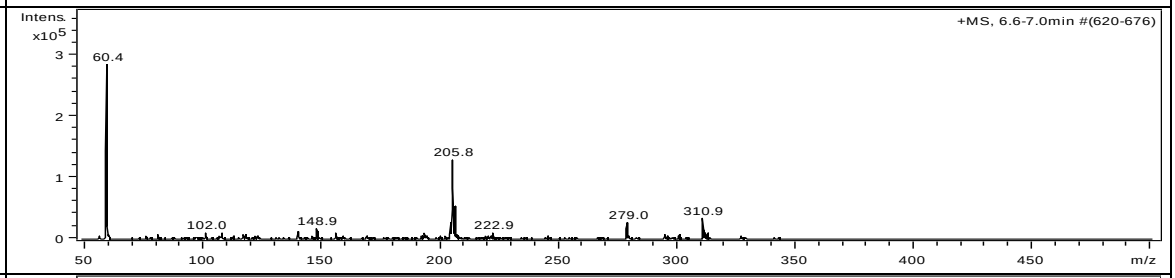
3	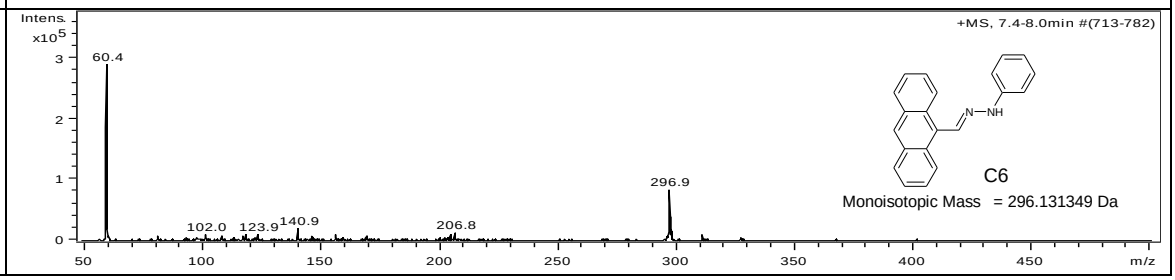

Figure SI 4.4.2. UV-chromatogram (254 nm) of bulk reaction of A2 and B3 measured with Agilent XCT LC system.

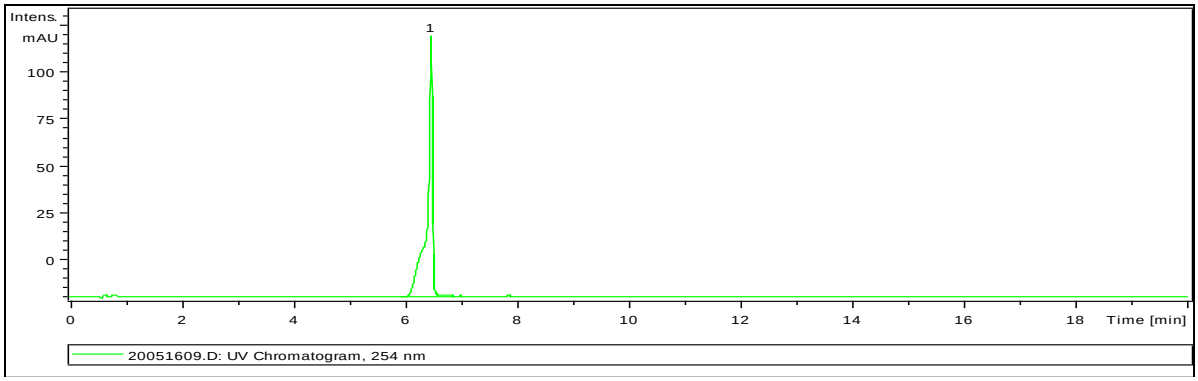

Table SI 4.4.2. Detailed MS data of bulk reaction of A2 and B3.

	MS spectrum
1	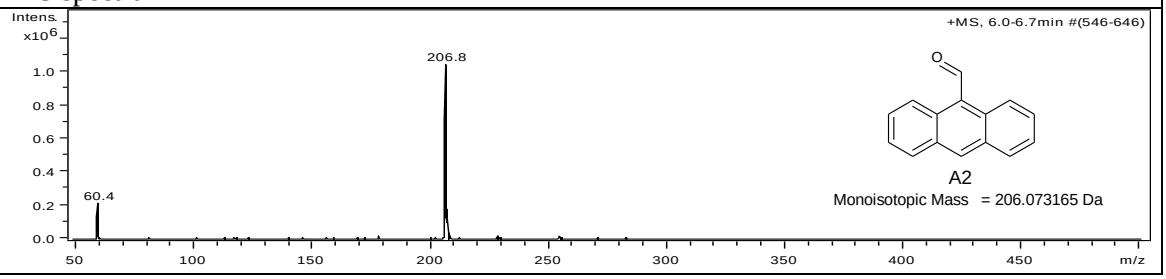

SI 4.5. Cinnamaldehyde (A3) + 4-Aminobiphenyl (B1)

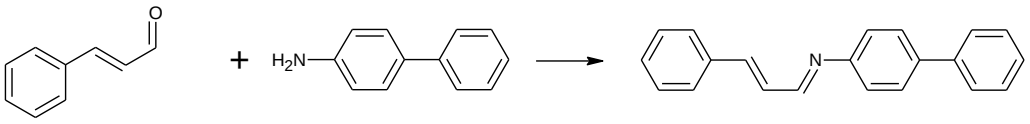

Figure SI 4.5.1. UV-chromatogram (254 nm) of ES reaction of A3 and B1 measured with Agilent XCT LC system.

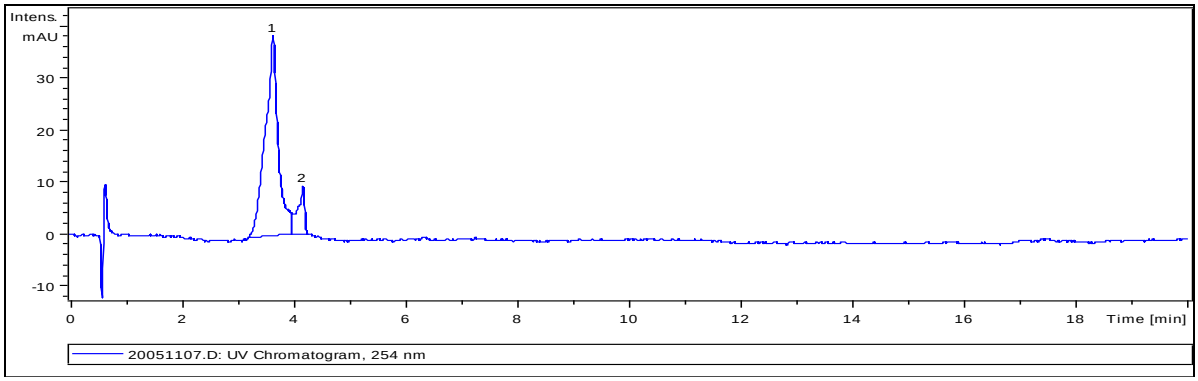

Table SI 4.5.1. Detailed MS data of ES reaction of A3 and B1.

	MS spectrum
1	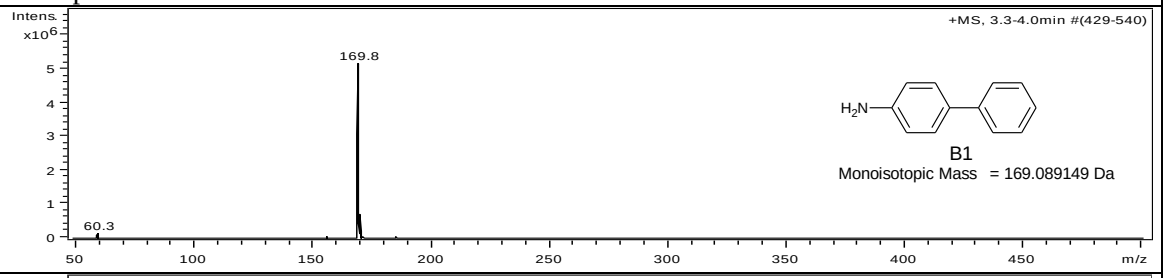
2	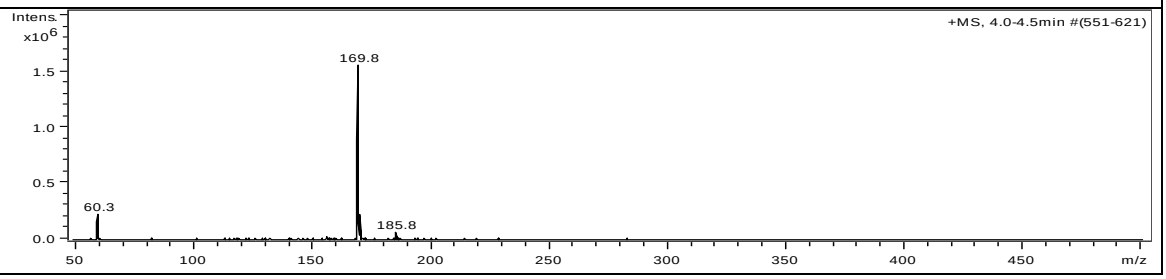

Figure SI 4.5.2. UV-chromatogram (254 nm) of bulk reaction of A3 and B1 measured with Agilent XCT LC system.

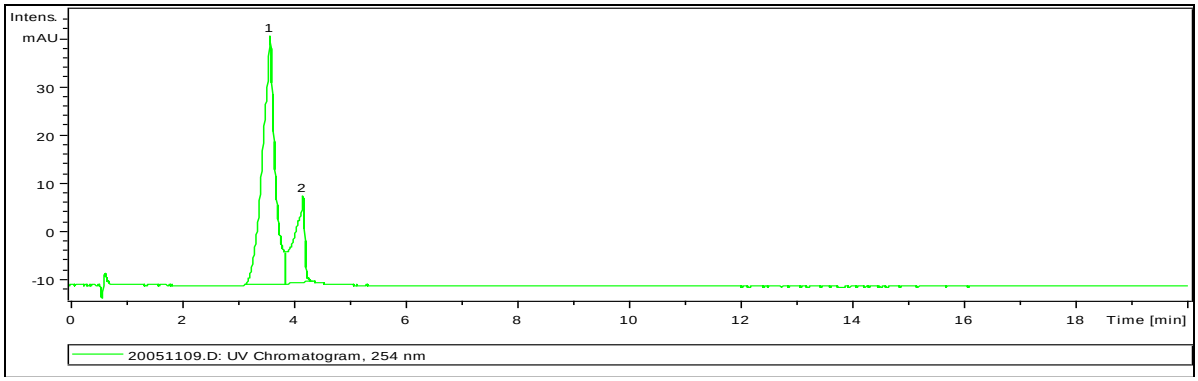

Table SI 4.5.2. Detailed MS data of bulk reaction of A3 and B1.

	MS spectrum
1	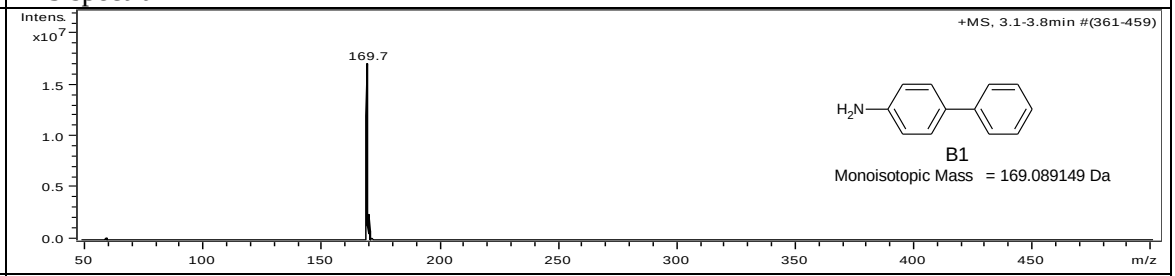
2	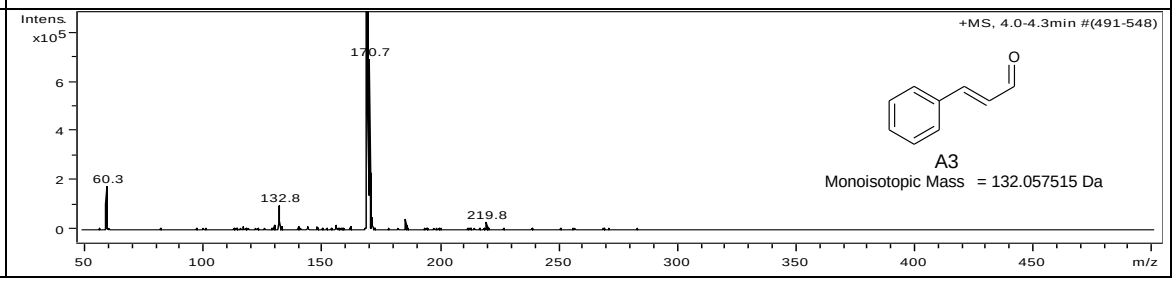

SI 4.6. Cinnamaldehyde (A3) + Phenylhydrazine (B3)

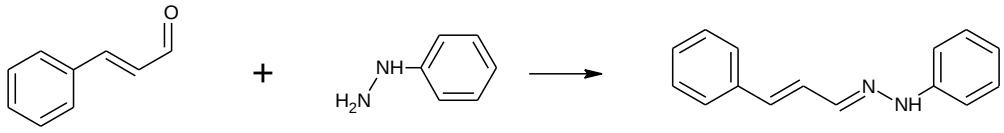

A3 B3 C9

Figure SI 4.6.1. UV-chromatogram (254 nm) of ES reaction of A3 and B3 measured with Agilent XCT LC system.

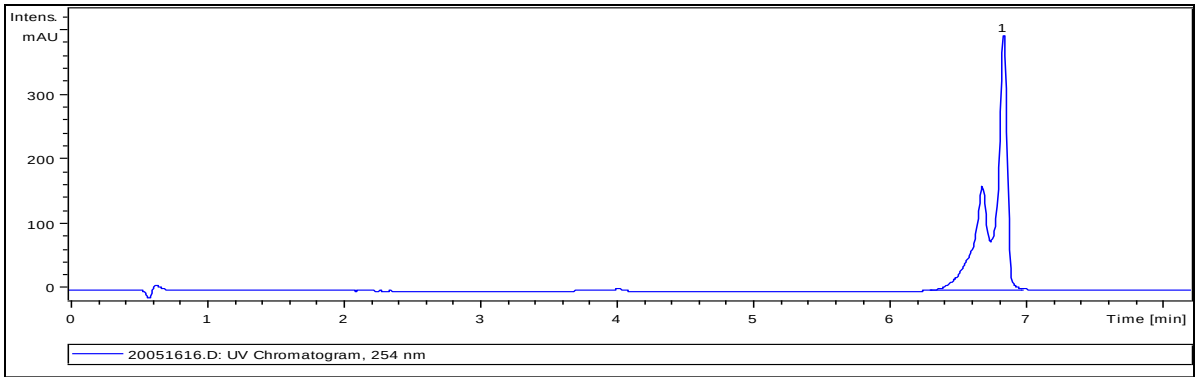

Table SI 4.6.1. Detdetailed MS data of ES reaction of A3 and B3.

	MS spectrum
1	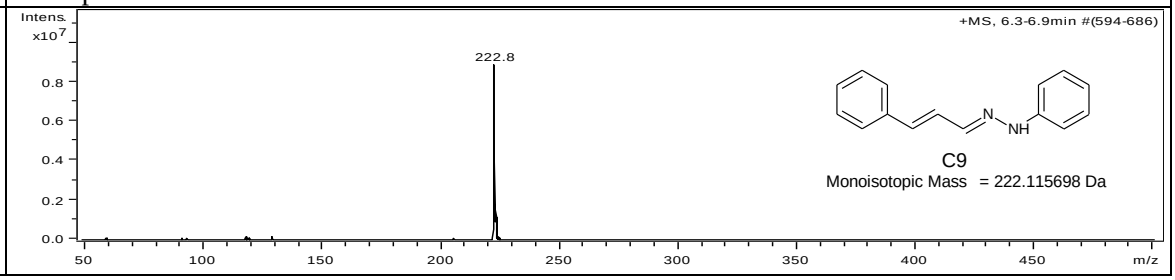

Figure SI 4.6.2. UV-chromatogram (254 nm) of bulk reaction of A3 and B3 measured with Agilent XCT LC system.

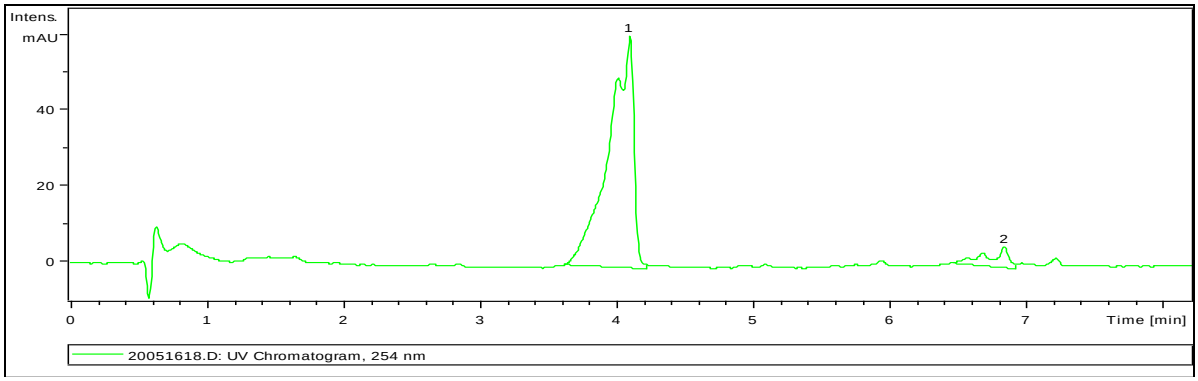

Table SI 4.6.2. Detailed MS data of bulk reaction of A3 and B3.

	MS spectrum
1	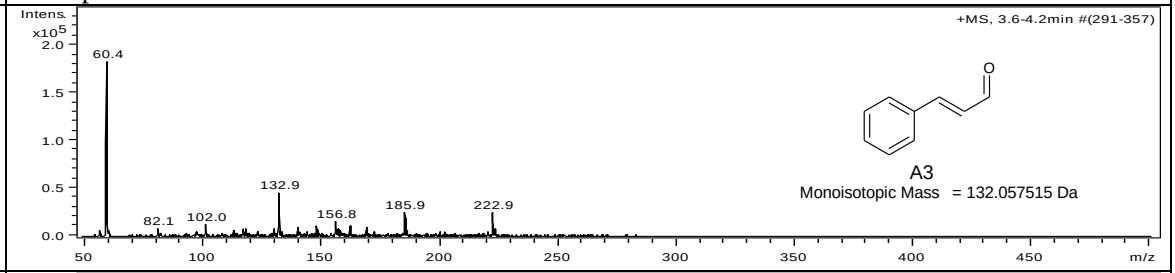
2	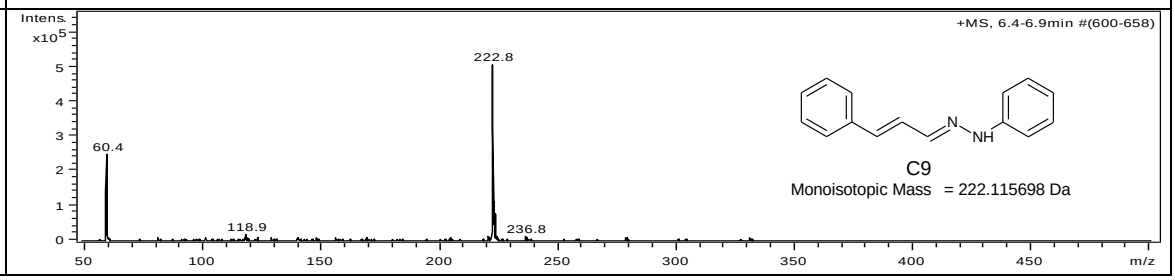

SI 4.7. 2,4,6-Triphenylpyrylium Tetrafluoroborate (A4) + 4-Aminobiphenyl (B1)

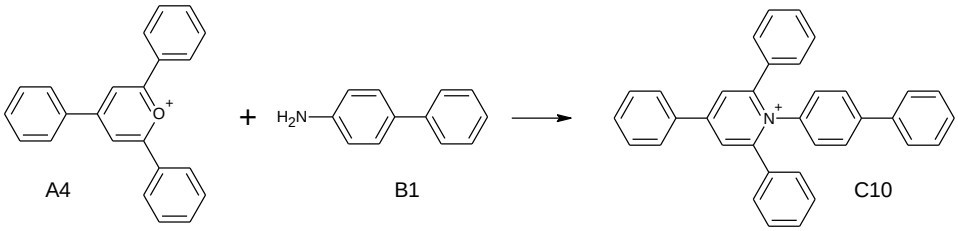

Figure SI 4.7.1. UV-chromatogram (254 nm) of ES reaction of A4 and B1 measured with Agilent QQQ LC system.

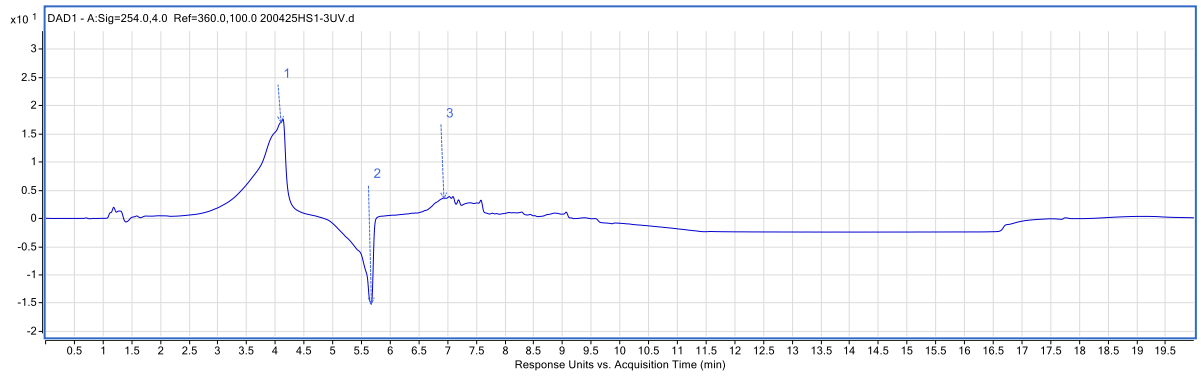

Table SI 4.7.1. Detailed MS data of ES reaction of A4 and B1.

	MS spectrum
1	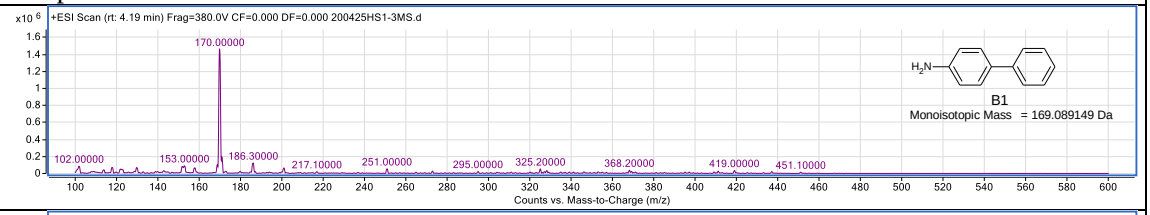
2	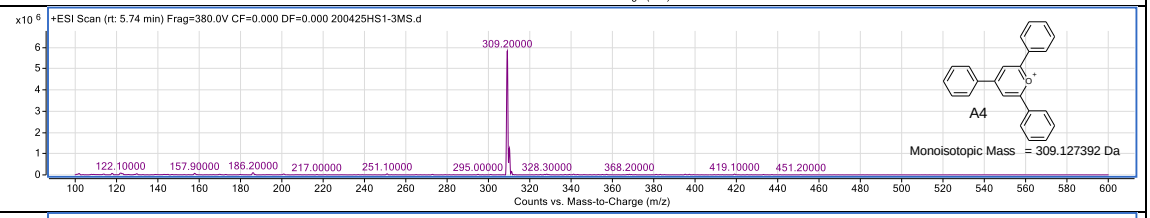
3	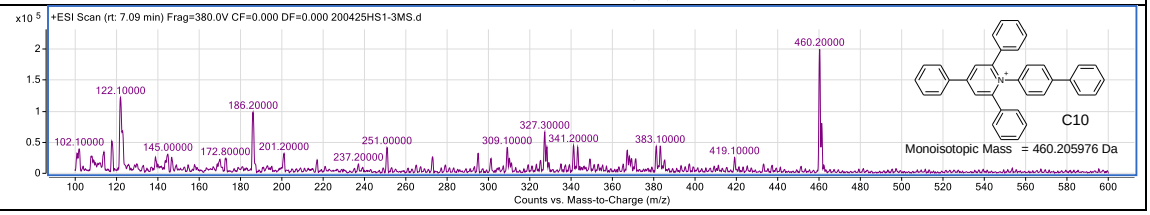

Figure SI 4.7.2. UV-chromatogram (254 nm) of bulk reaction of A4 and B1 measured with Agilent QQQ LC system.

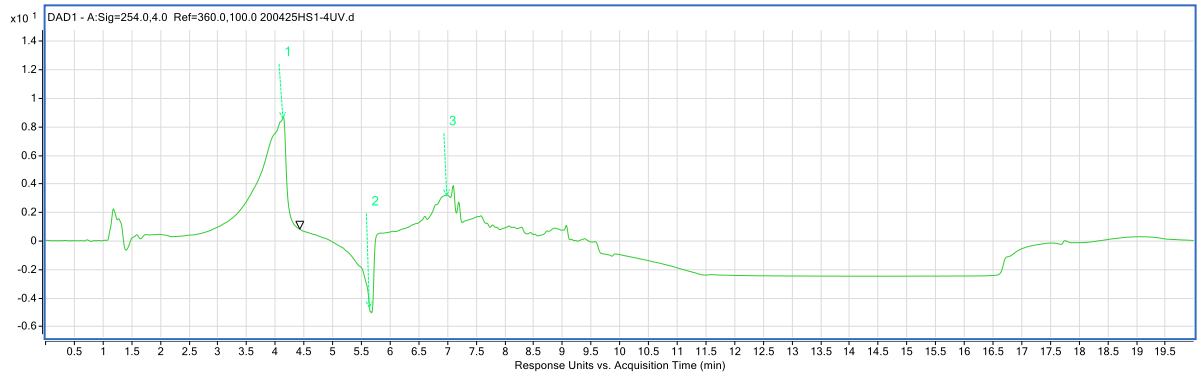

Table SI 4.7.2. Detailed MS data of bulk reaction of A4 and B1.

	MS spectrum
1	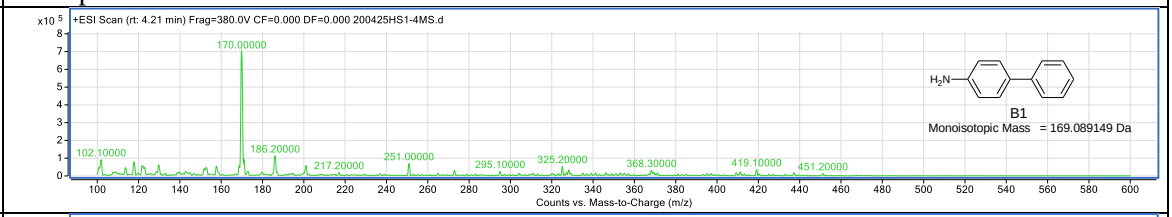
2	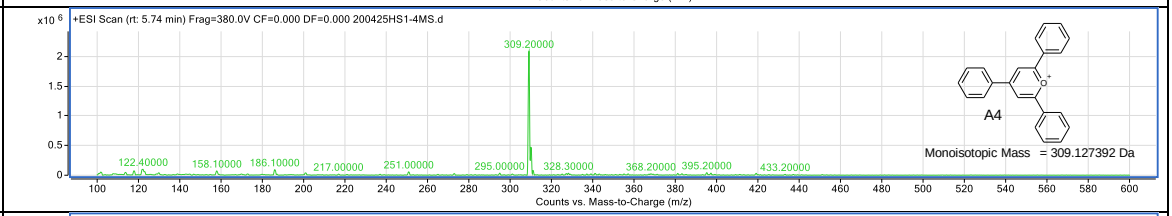
3	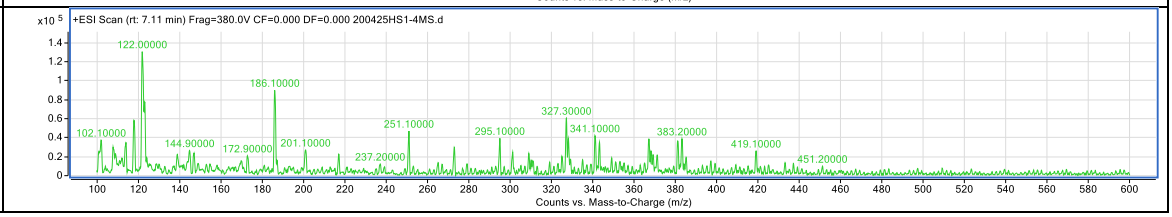

SI 4.8. 2,4,6-Triphenylpyrylium Tetrafluoroborate (A4) + 2-Aminofluorene (B2)

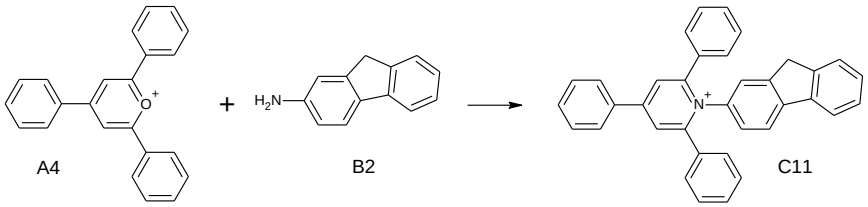

Figure SI 4.8.1. UV-chromatogram (254 nm) of ES reaction of A4 and B2 measured with Agilent XCT LC system.

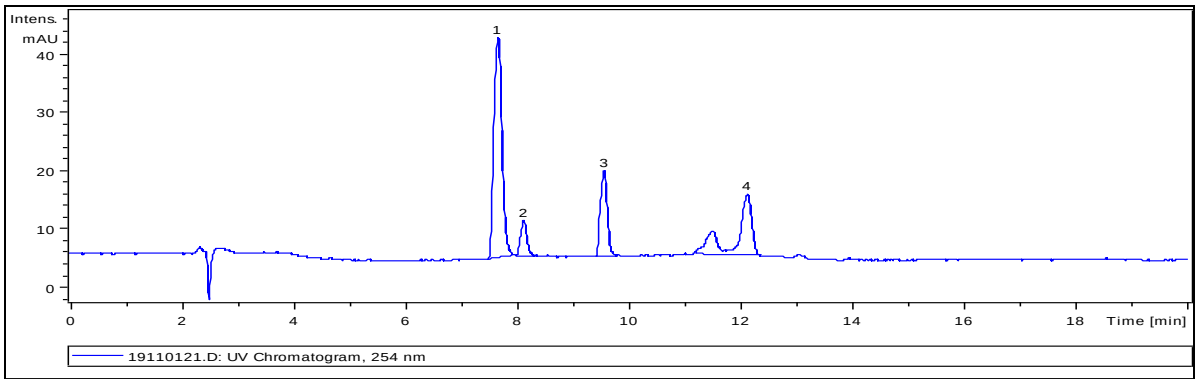

Table SI 4.8.1. Detailed MS data of ES reaction of A4 and B2.

	MS spectrum
1	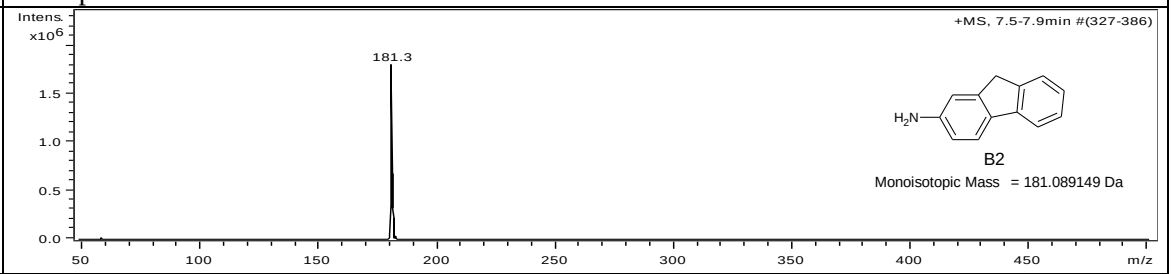
2	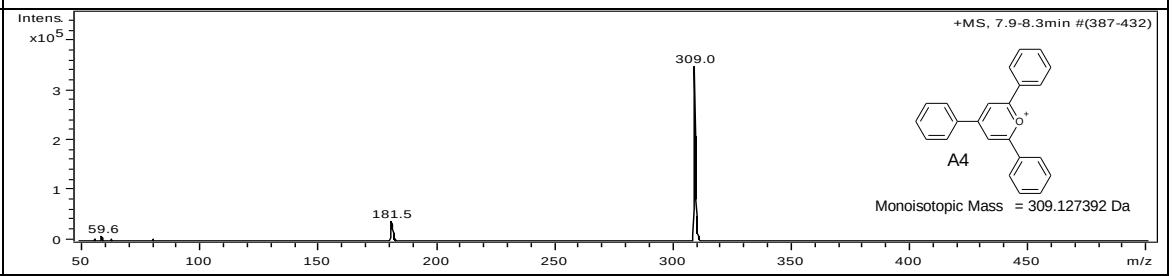
3	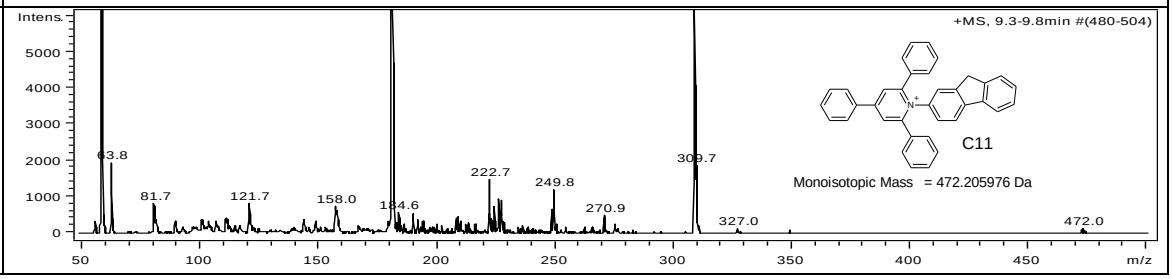

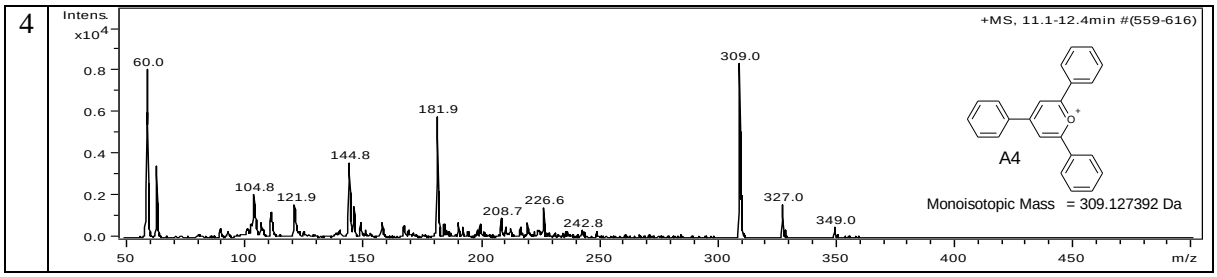

Figure SI 4.8.2. UV-chromatogram (254 nm) of bulk reaction of A4 and B2 measured with Agilent XCT LC system.

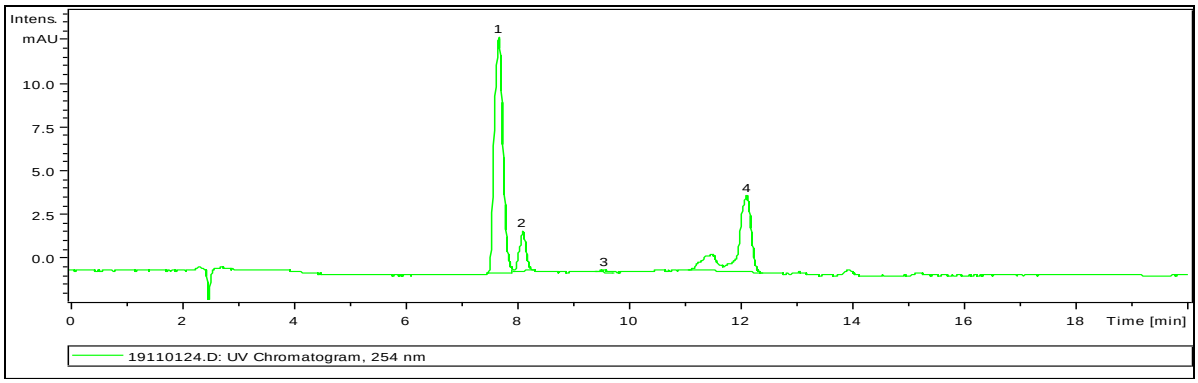

Table SI 4.8.2. Detailed MS data of bulk reaction of A4 and B2.

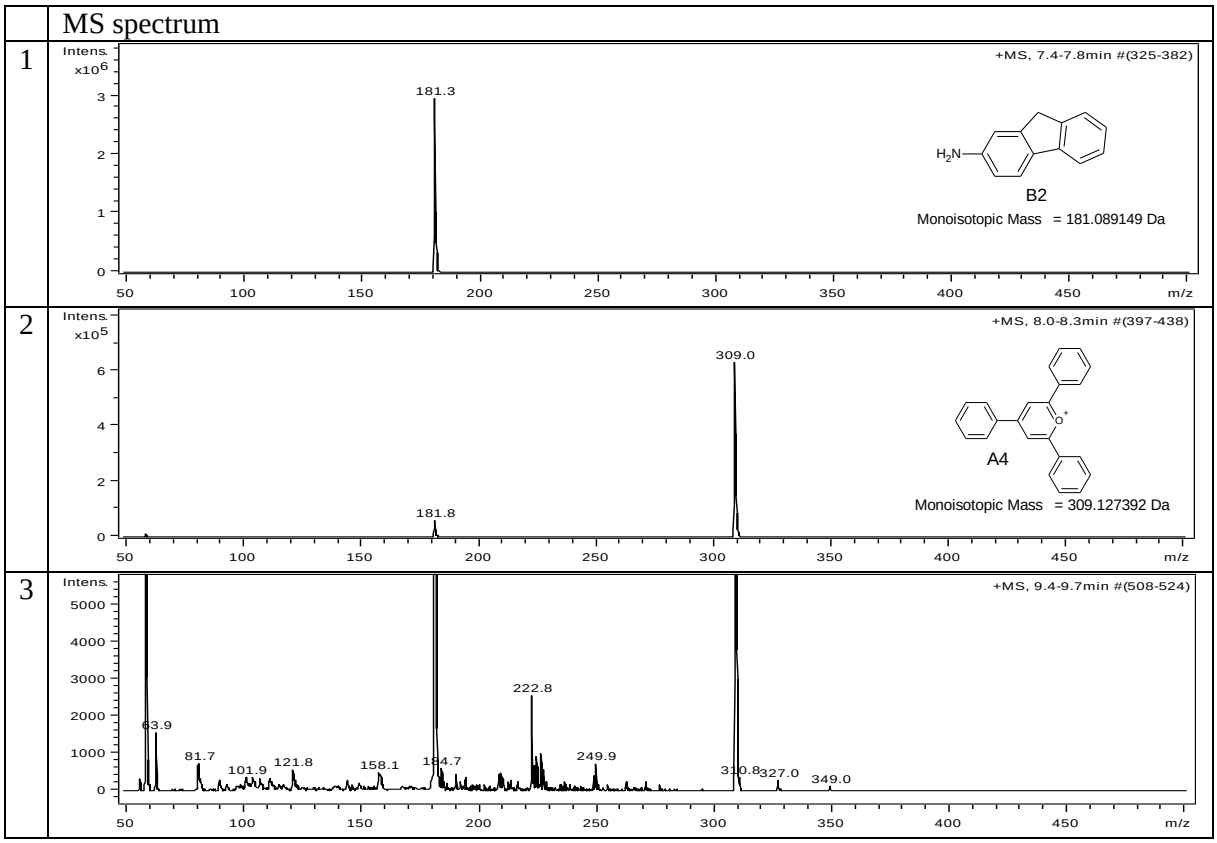

4	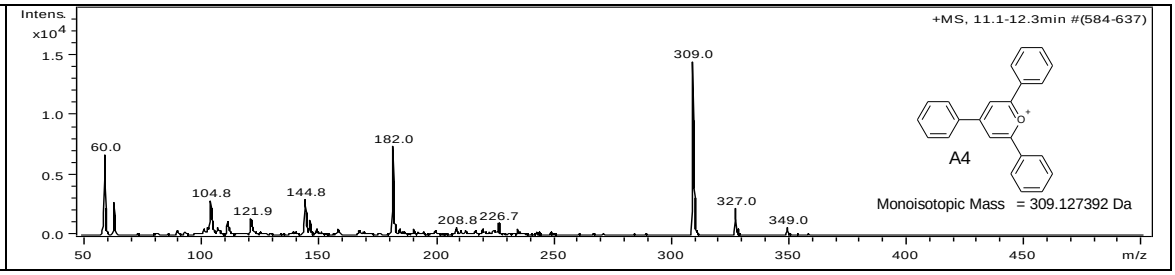

Intens.
x10^4
1.5
1.0
0.5
0.0
60.0
104.8
121.9
144.8
182.0
208.8
226.7
309.0
327.0
349.0
50
100
150
200
250
300
350
400
450
m/z
+MS, 11.1-12.3min #(584-637)
A4
Monoisotopic Mass = 309.127392 Da

SI 4.9. 1-(2,4-dinitrophenyl)-4-(pyridine-4-yl)pyridinium chloride (A5) + 4-Aminobiphenyl (B1)

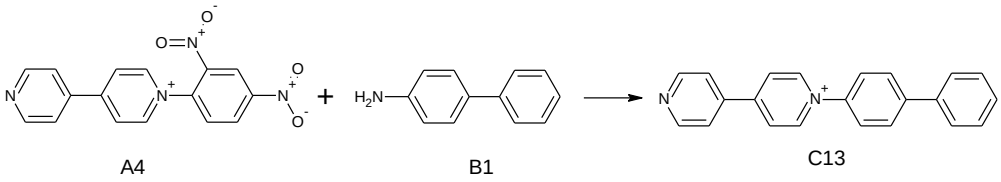

Figure SI 4.9.1. UV-chromatogram (254 nm) of ES reaction of A5 and B1 measured with Agilent XCT LC system.

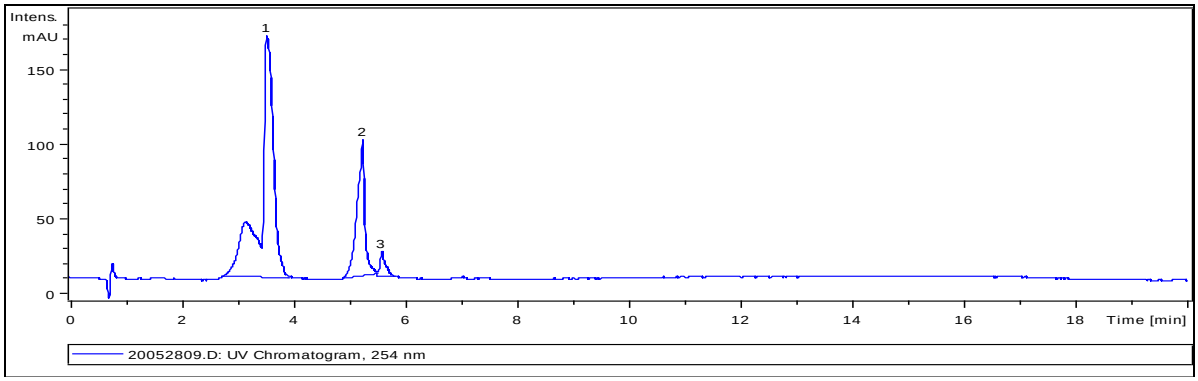

Table SI 4.9.1. Detailed MS data of ES reaction of A5 and B1.

	MS spectrum
1	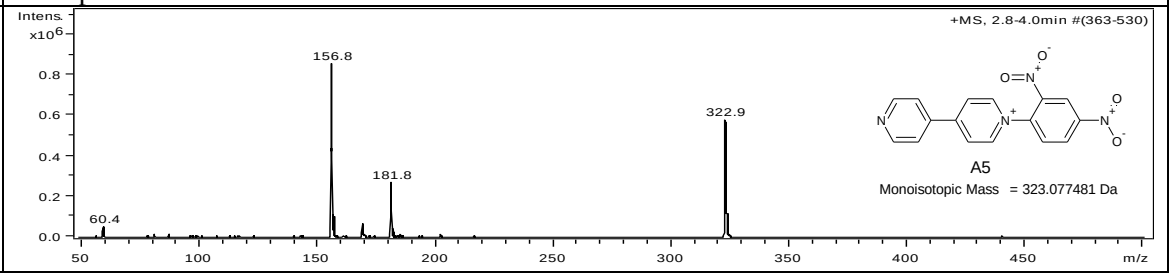
2	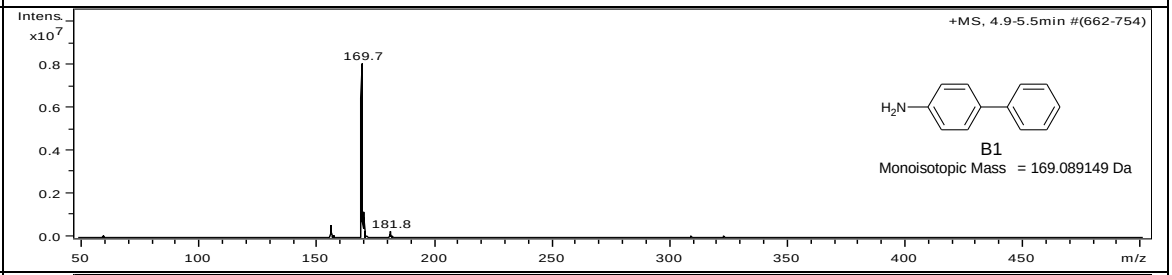
3	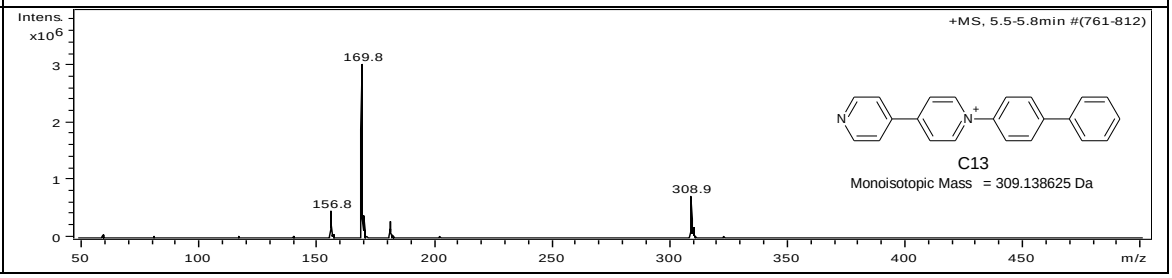

Figure SI 4.9.2. UV-chromatogram (254 nm) of bulk reaction of A5 and B1 measured with Agilent XCT LC system.

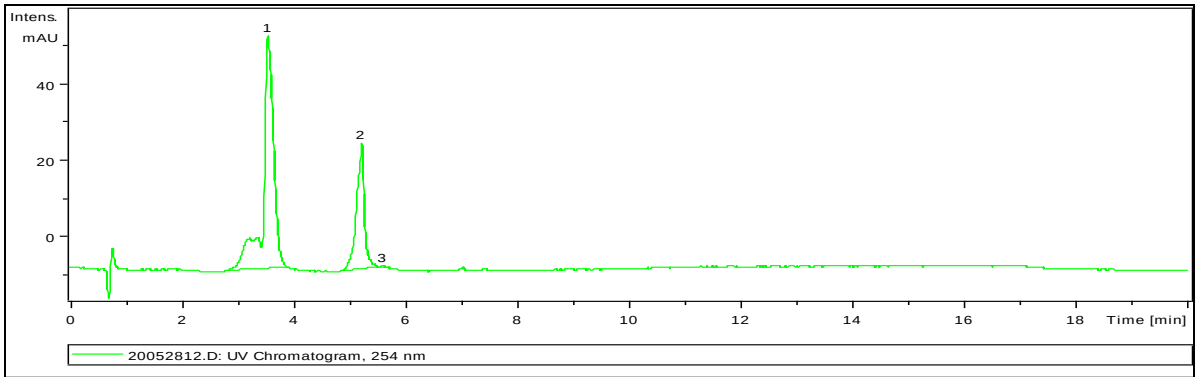

Table SI 4.9.2. Detailed MS data of bulk reaction of A5 and B1.

	MS spectrum
1	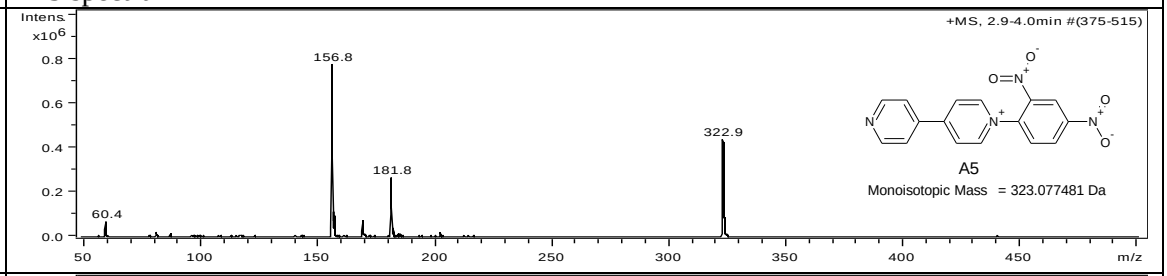
2	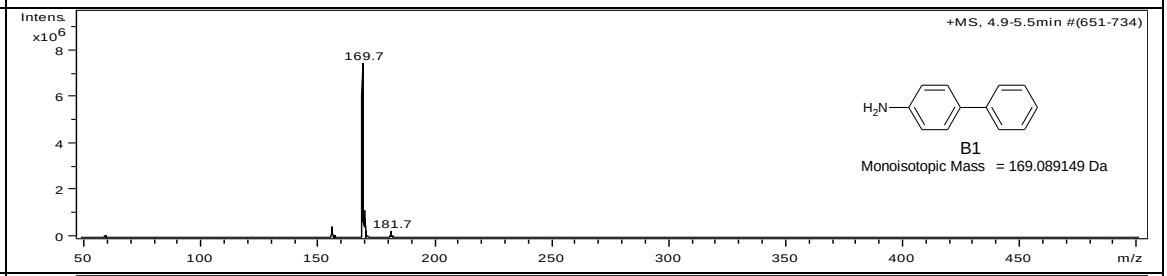
3	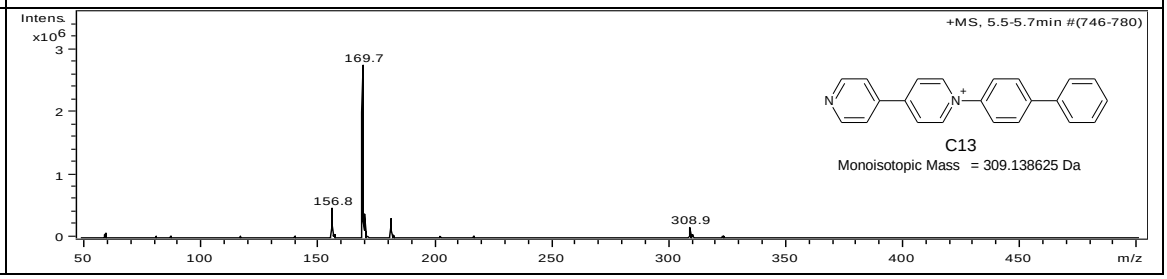

SI 4.10. 1-(2,4-dinitrophenyl)-4-(pyridine-4-yl)pyridinium chloride (A5) + 2-Aminofluorene (B2)

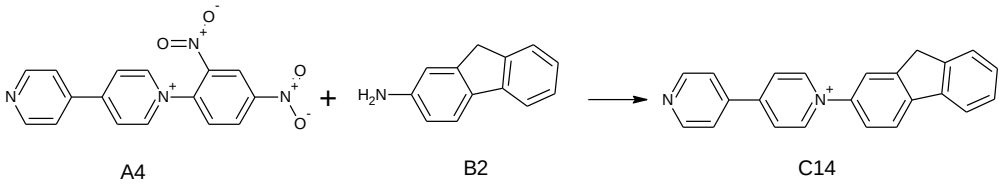

Figure SI 4.10.1. UV-chromatogram (254 nm) of ES reaction of A5 and B2 measured with Agilent XCT LC system.

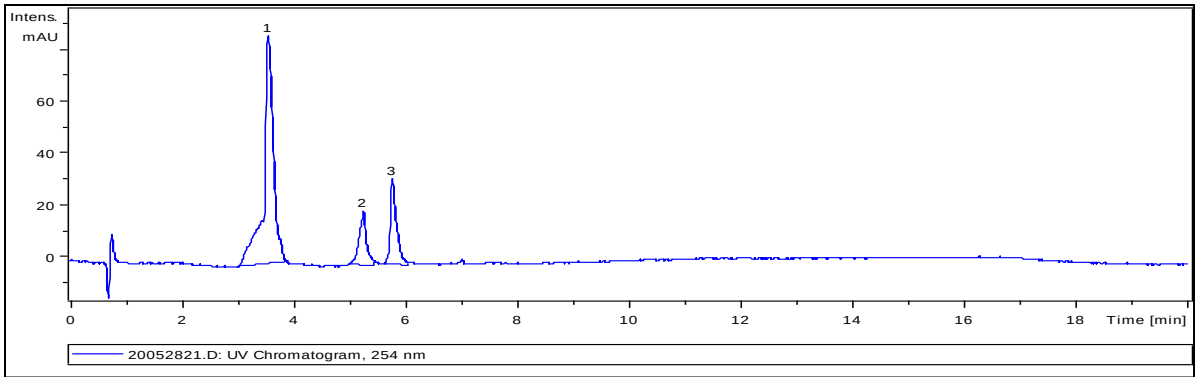

Table SI 4.10.1. Detailed MS data of ES reaction of A5 and B2.

	MS spectrum
1	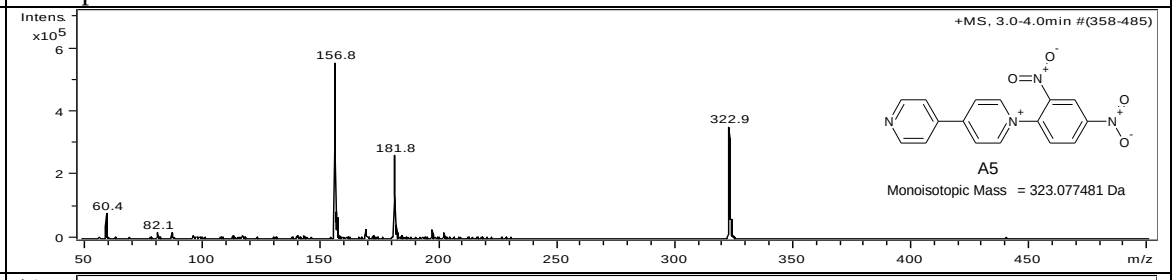
2	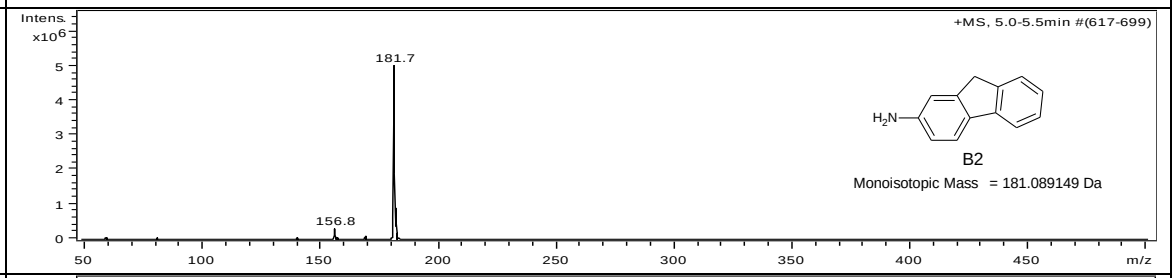
3	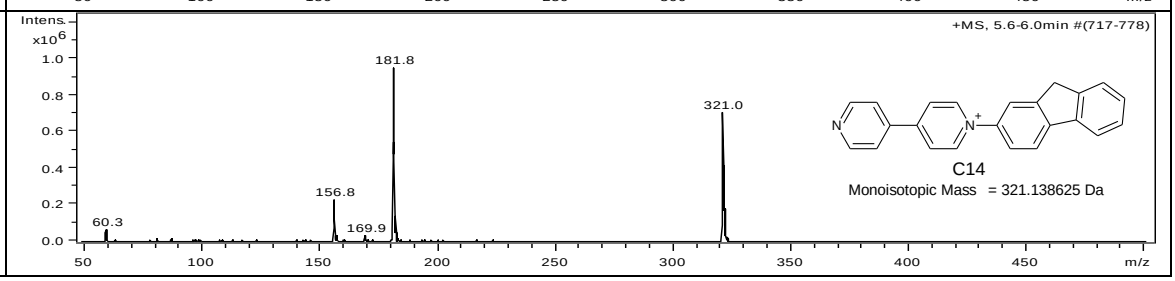

Figure SI 4.10.2. UV-chromatogram (254 nm) of bulk reaction of A5 and B2 measured with Agilent XCT LC system.

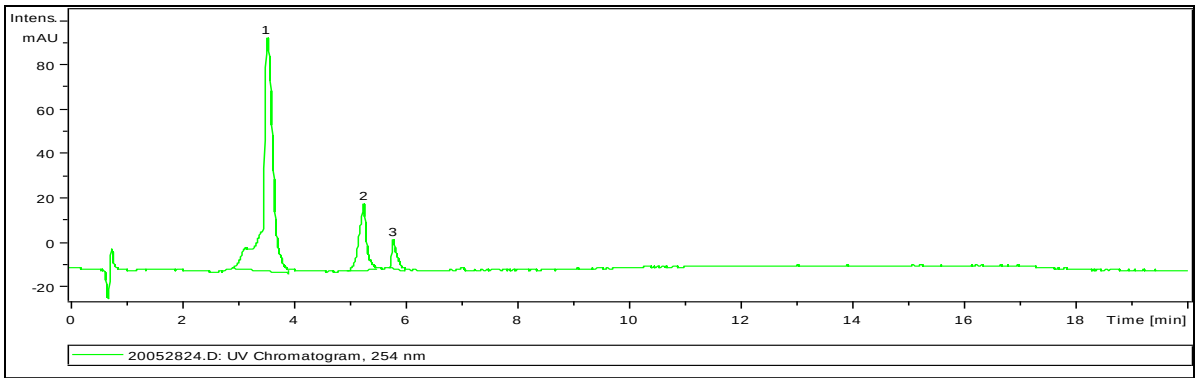

Table SI 4.10.2. Detailed MS data of bulk reaction of A5 and B2.

	MS spectrum
1	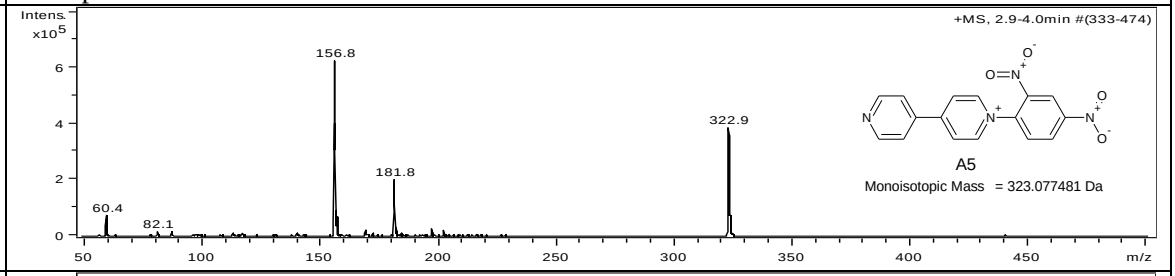
2	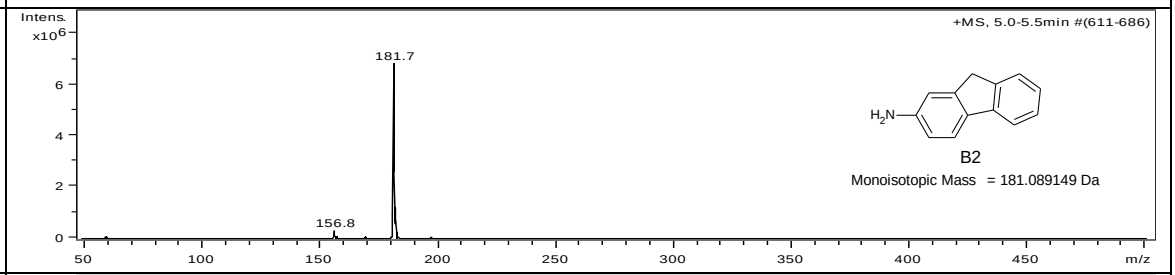
3	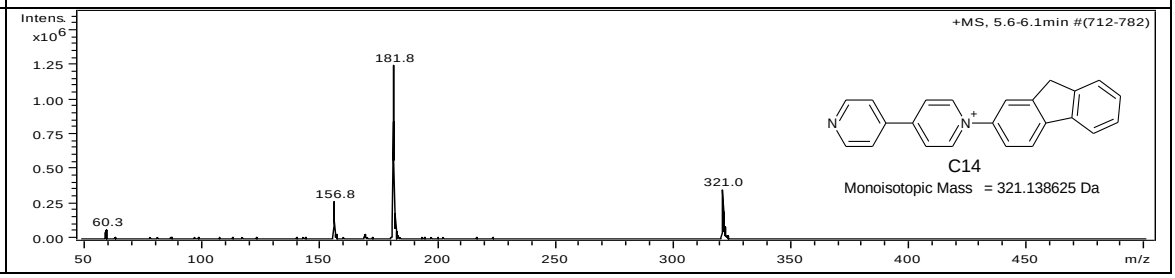

SI 4.11. 1-(2,4-dinitrophenyl)-4-(pyridine-4-yl)pyridinium chloride (A5) + Phenylhydrazine (B3)

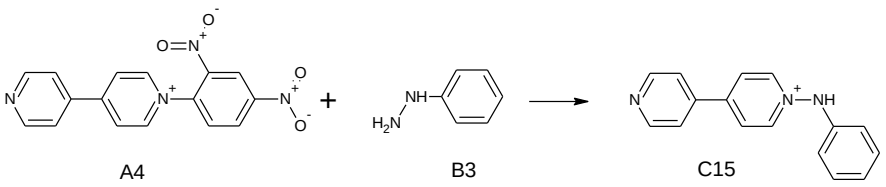

Figure SI 4.11.1. UV-chromatogram (254 nm) of bulk reaction of A5 and B3 measured with Agilent XCT LC system.

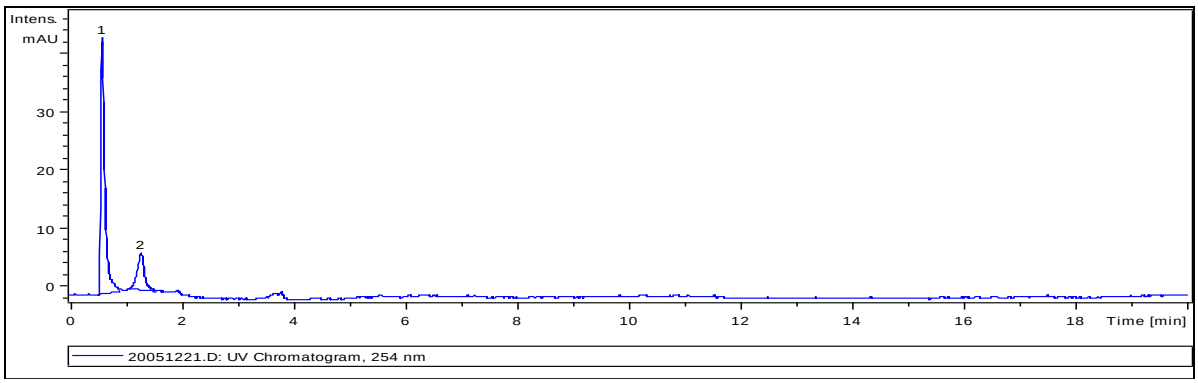

Table SI 4.11.1. Detailed MS data of bulk reaction of A5 and B3.

	MS spectrum
1	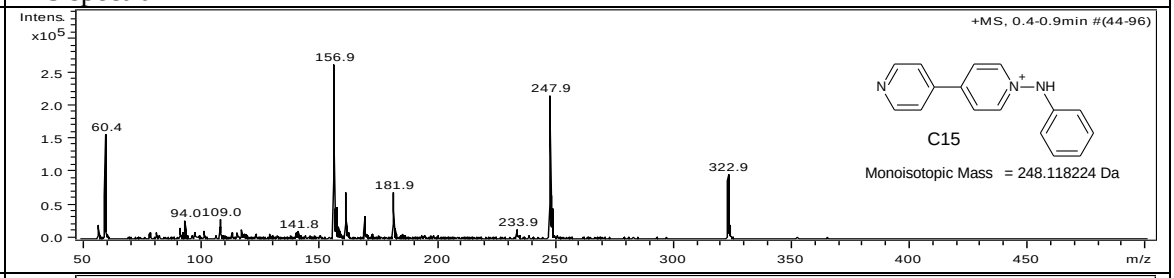
2	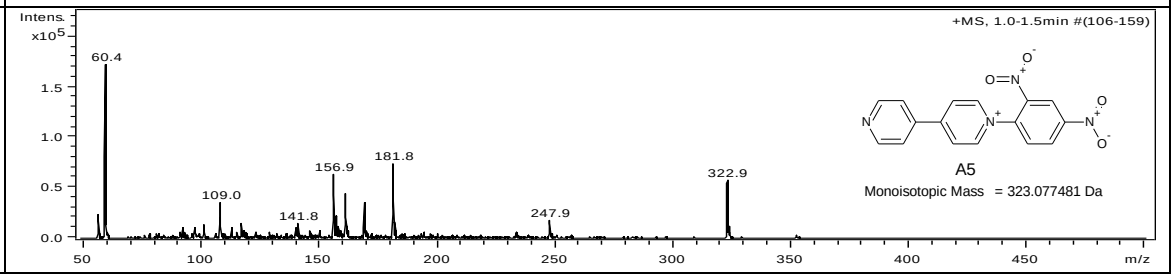

Figure SI 4.11.2. UV-chromatogram (254 nm) of bulk reaction of A5 and B3 measured with Agilent XCT LC system.

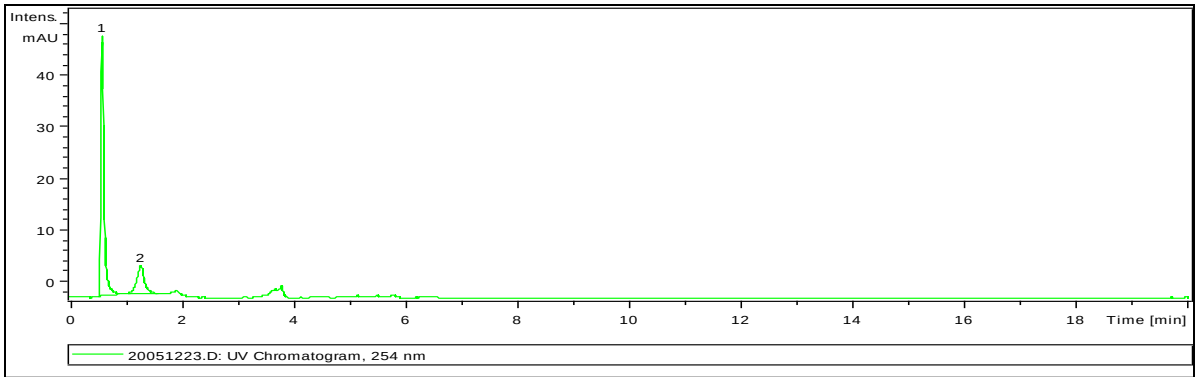

Table SI 4.11.2. Detailed MS data of bulk reaction of A5 and B3.

	MS spectrum
1	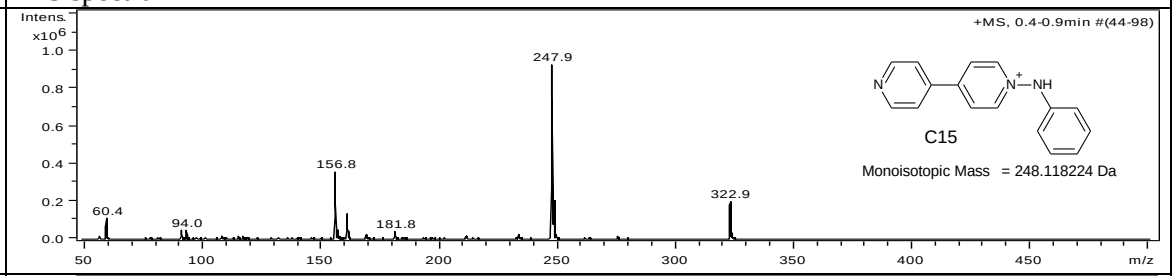
2	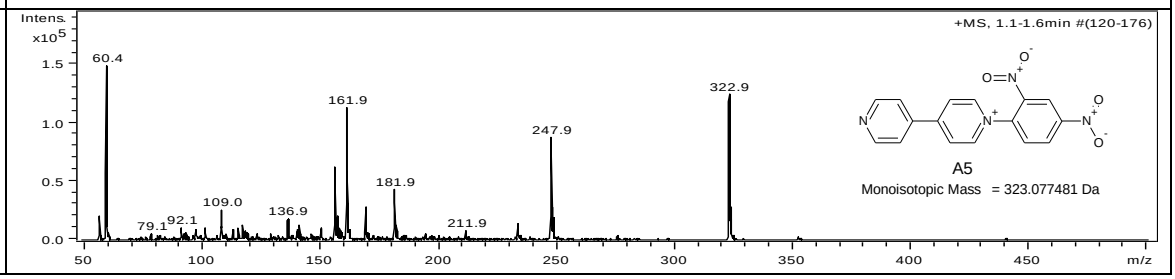

SI 5. Fluorescence Emission Spectra

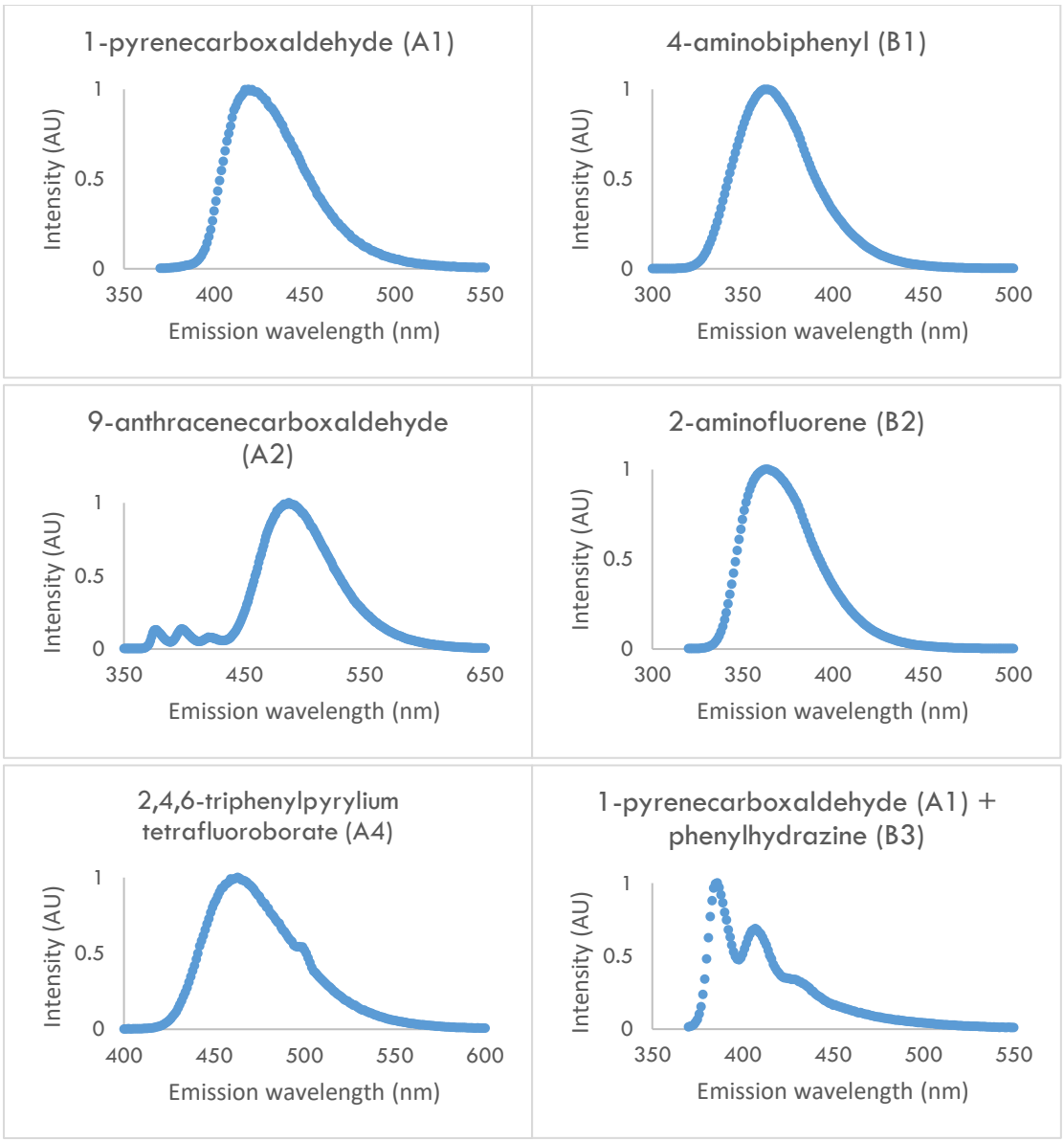

SI 5.1. Fluorescence Emission Spectra of Two Zincke Reactions (y-axis magnified for graphs on the right side)

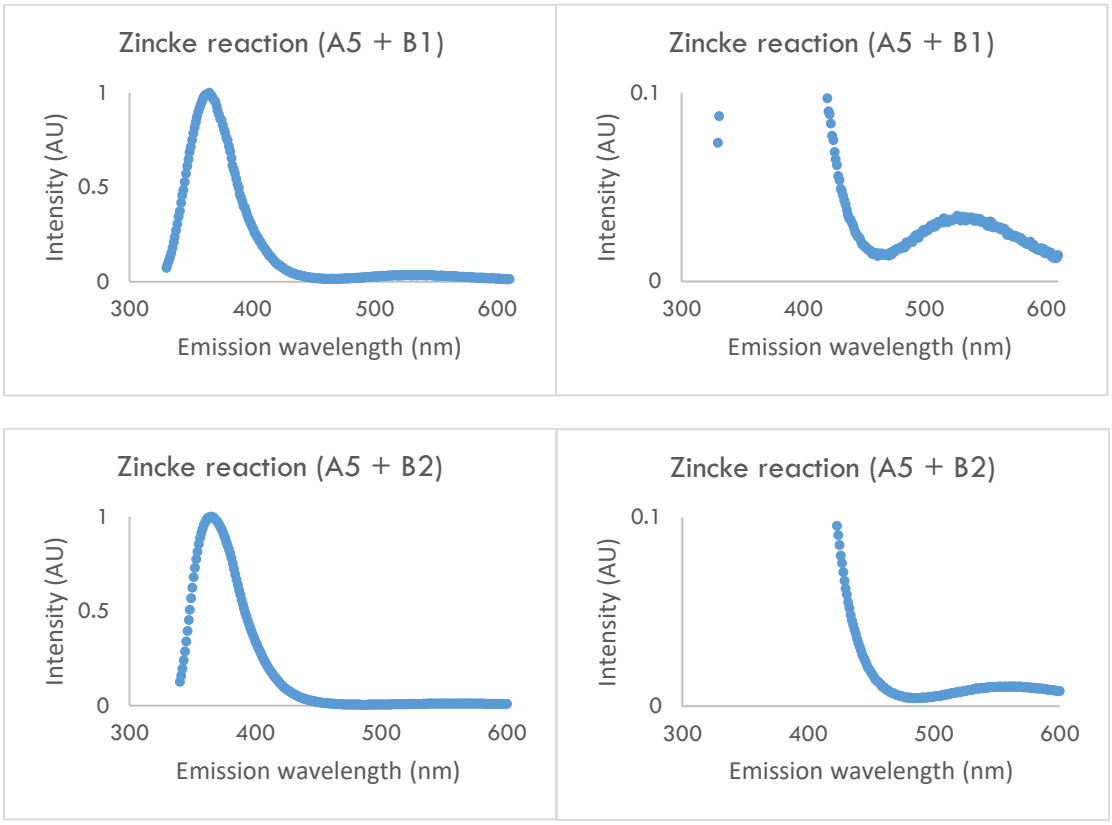

SI 6. Measuring Kinetics with NMR

SI 6.1. NMR Spectrum of 2-Aminofluorene (B2).

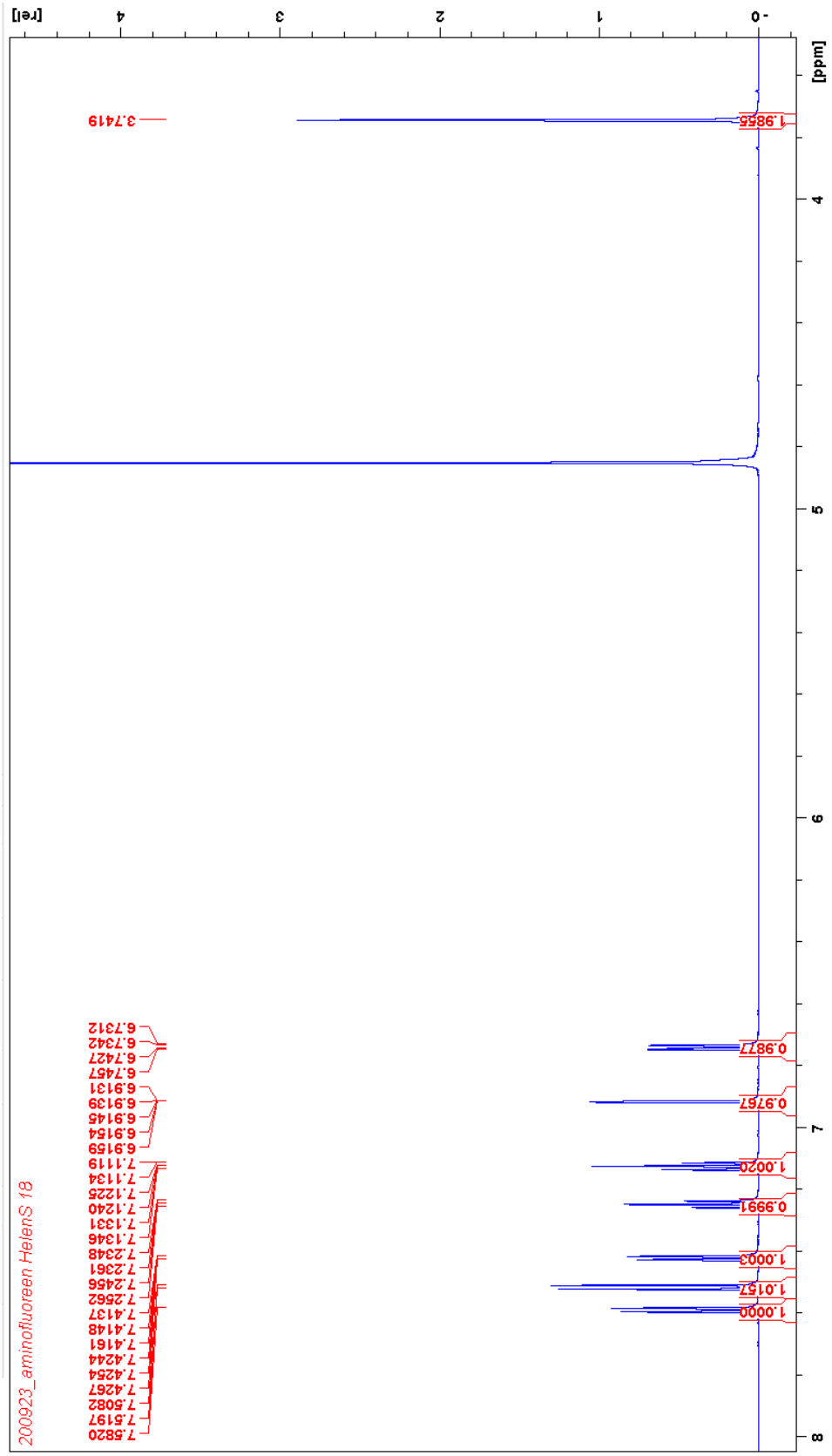

SI 6.2. NMR Spectra of Reaction Mixture between A5 and B2 Measured at 1, 5, 10, 15 and 20 min.

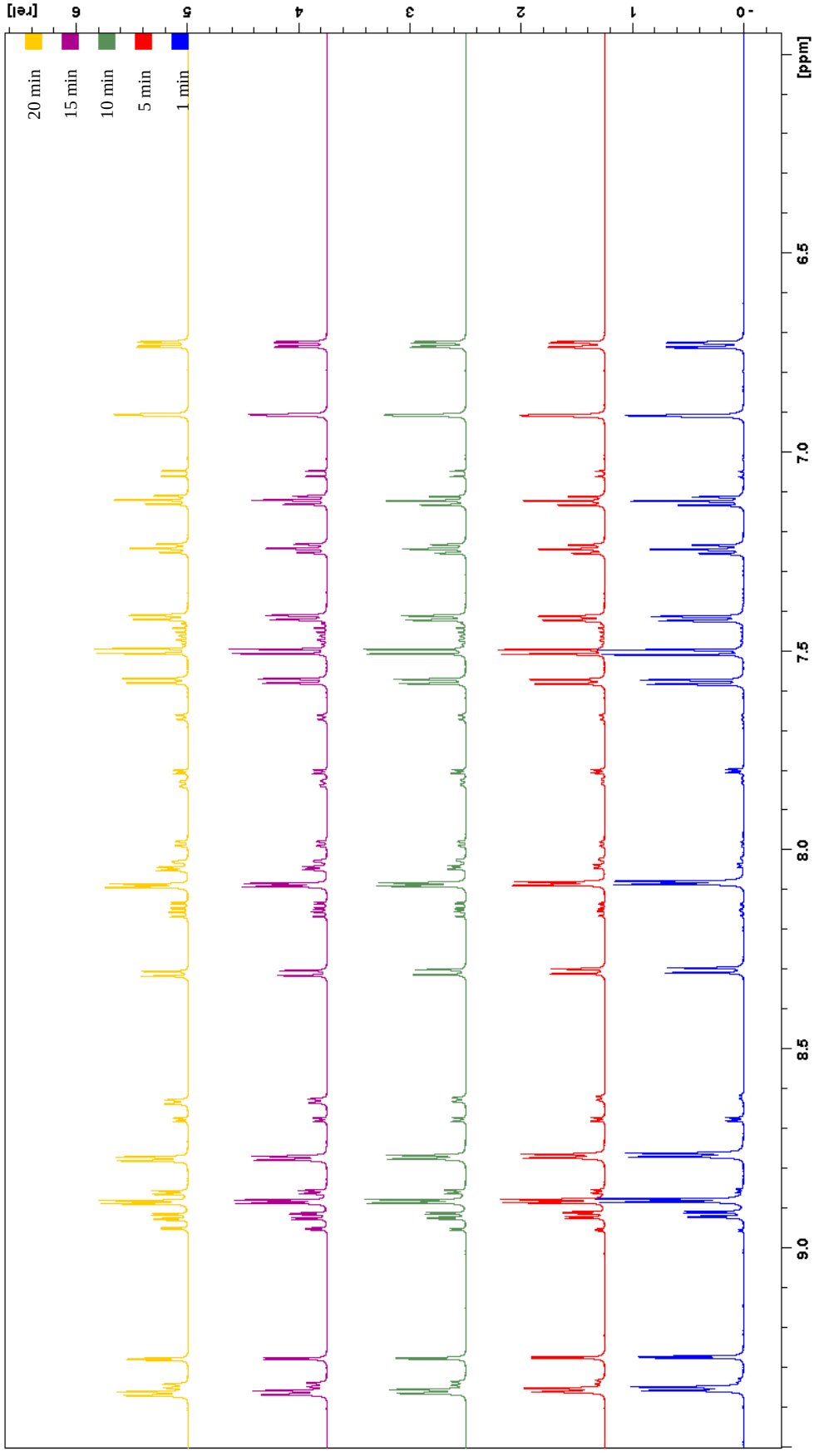

Non-exclusive licence to reproduce thesis and make thesis public

I, Helen Sepman

1. herewith grant the University of Tartu a free permit (non-exclusive licence) to reproduce, for the purpose of preservation, including for adding to the DSpace digital archives until the expiry of the term of copyright, “Investigation of Fluorescent Reactions in Charged Droplets for Reaction Kinetics Monitoring” supervised by Andi Kipper and Anneli Kruve.

2. I grant the University of Tartu a permit to make the work specified in p. 1 available to the public via the web environment of the University of Tartu, including via the DSpace digital archives, under the Creative Commons licence CC BY NC ND 3.0, which allows, by giving appropriate credit to the author, to reproduce, distribute the work and communicate it to the public, and prohibits the creation of derivative works and any commercial use of the work until the expiry of the term of copyright.

3. I am aware of the fact that the author retains the rights specified in p. 1 and 2.

4. I certify that granting the non-exclusive licence does not infringe other persons’ intellectual property rights or rights arising from the personal data protection legislation.

Helen Sepman

04.06.2021